Nano-MoO2 activates peroxymonosulfate for the degradation of PAH derivatives

(Article begins on next page)

03 June 2024

Nano MoO$_2$ as a novel catalyst to activate peroxymonosulfate for degradation of naphthalene and its derivatives

Xuwen Chen[a], Pengfei Cheng[a], Davide Vione[b], Xuqiang Zhao[a], Chao Qin[a], Yanzheng Gao [a],*

[a] Institute of Organic Contaminant Control and Soil Remediation, College of Resources and Environmental Sciences, Nanjing Agricultural University, Nanjing 210095, China.

[b] Department of Chemistry, University of Torino, Via Pietro Giuria 5, 10125 Torino, Italy.

*****Corresponding author:** Yanzheng Gao.

Address: Weigang Road 1, Nanjing 210095, China.

ORCID No.: 0000-0002-3814-3555

Tel: +86-25-84395019.

E-mail: gaoyanzheng@njau.edu.cn, gaosoil@163.com.

Abstract

In recent years, many people have paid attention to the removal of PAHs and their derivatives to face huge challenges of environmental safety. Novel nano MoO_2 was here employed for the first time as an environmentally friendly catalyst to activate peroxymonosulfate (PMS) for the removal of toxic contaminants. In particular, we studied the nano-MoO_2-induced PMS activation for the degradation of naphthalene and of derivatives such as 1-methylnaphthalene, 1-nitronaphthalene, 1-chloronaphthalene, 1-naphthylamine, and 1-naphthol. Interestingly, the degradation of naphthalene was often more efficient compared to those of the substituted compounds. The amount of nano MoO_2 was the main factor that affected contaminant removal, followed by the dose of PMS and the suspension pH. Electron paramagnetic resonance (EPR) spectroscopy revealed that $SO_4^{\bullet-}$, $^{\bullet}OH$, $O_2^{\bullet-}$ and $^1O_2$ were formed in the system, but $SO_4^{\bullet-}$ and $^{\bullet}OH$ were mainly involved in the degradation of the target compounds. A major exception was 1-naphthylamine, which was efficiently degraded by reaction with PMS alone, while the degradation of 1-naphthol mainly depended on $SO_4^{\bullet-}$. X-ray photoelectron spectroscopy (XPS) determined the transformation of Mo(IV) into Mo(V) and Mo(VI), and proved that the activation process between nano MoO_2 and PMS proceeded by electron transfer. Furthermore, Mo(IV) can be regenerated from the reduction of Mo(VI) on the surface of nano MoO_2. The degradation intermediates of the target pollutants were identified, thereby allowing for the proposal of possible degradation pathways.

Keywords

1. Introduction

Polycyclic Aromatic Hydrocarbons (PAHs) are a class of toxic organic pollutants containing two or more benzene rings. Some of them have also mutagenic and carcinogenic properties [1]. Natural and substituted PAHs (SPAHs) arise from the incomplete combustion of carbon-containing compounds and materials and from other industrial processes, and they are discharged and accumulated in the atmosphere as well as soil and water environments [2, 3]. Sixteen PAHs (EPA-PAHs) have been classified by the United States Environmental Protection Agency (US EPA) as priority controlled pollutants [4]. According to the World Health Organization, the levels of carcinogenic benzo(a)pyrene in drinking water should not exceed 10 ng/L, and the levels of other PAHs should not exceed 200 ng/L [5].

Both PAHs and SPAHs occur in the natural environment [6]. SPAHs can be directly discharged into the environment by incomplete combustion, or can be formed from the parent PAHs by chemical or microbial action [7, 8]. Indeed, under certain conditions one or several hydrogen atoms in PAHs might be substituted by functional groups such as methyl, nitro, halogen, amino and hydroxyl, to form for instance methyl-PAHs, nitro-PAHs, chloro-PAHs, amino-PAHs and hydroxy-PAHs. Because many SPAHs have higher toxicity than the parent PAHs, SPAHs have received increasing attention in recent years, due to their potential to damage both ecosystems and human health [2, 9].

Naphthalene is one of the 16 priority PAHs, and its derivatives such as methylnaphthalene, nitronaphthalene, chloronaphthalene, naphthylamine and naphthol are

also widely present in the environment. Having water solubility of 31 mg/L, naphthalene can easily cause water pollution. Its exposure threshold limit in the atmosphere is 50 $\mu g/m^3$, which has been far exceeded in several circumstances [10]. Moreover, coal combustion has been shown to produce methyl-PAHs in amounts that are of the same order of magnitude as the priority PAHs [11]. This finding is of particular concern, because alkylated PAHs are more toxic than non-alkylated PAHs and cause inflammatory diseases and cancer [12]. Nitro-PAHs such as nitro-naphthalene can be formed during incomplete combustion [13], but also by the reaction of PAHs with nitrogen oxides in polluted air [14]. The mutagenicity of nitro-PAHs is 10^5 times higher than that of the parent compounds, and the carcinogenicity is nearly 10 times higher [15]. Another SPAH, 1-chloronapthalene, is mainly formed in wastewater treatment plants [16, 17]. It is accumulated in sediments and the tissues of marine organisms, and its volatility ensures its occurrence in air where it has long half-life [18]. The potentially carcinogenic 1-naphthylamine is mainly emitted by dyes, photographic, pharmaceutical and agrochemical industries [19]. Toxic and non-biodegradable 1-naphthol is a precursor of the insecticide carbaryl [19], thus its use on the long term and on a wide scale can be very harmful for the environment.

Among the possible removal methods for PAHs, advanced oxidation processes (AOPs) has been widely investigated due to fast reaction and high efficiency [20]. Effective oxidants are permanganate [21], H_2O_2 [1], persulfate (PS) [22] and peroxymonosulfate (PMS) [23]. Among these oxidants, PMS or PS have been recently shown to be very effective reagents, with limited secondary pollution and good environmental friendliness

[24]. However, their direct depolluting action is quite poor, unless they are activated to generate more active oxidants such as sulfate and hydroxyl radicals (E ($SO_4^{\bullet-}$) = 2.5-3.1 V，E ($^{\bullet}OH$) = 1.8-2.7 V [25]). The activation of PMS and PS can occur under certain conditions, such as in the presence of heat [26], ultraviolet light [27], visible light [28], and transition metal compounds [29]. The latter are widely used because they do not require additional energy, and are also cheap and easy to obtain. Activation of PMS and PS has been reported to occur in the presence of compounds containing Fe [30], Co [25], Mn [31], Cu [32] etc., but some transition metal ions or oxides have not been explored. Moreover, there are presently few reports on the degradation of PAHs by activated PMS.

Molybdenum (Mo) is a transition metal element that is widely found in nature. It is also a trace element necessary for the human body, for animals and plants, where it plays an important role in growth and development [33]. The minerals containing Mo in nature are mainly molybdenite, wulfenite, and powellite [34]. The Mo oxidation states range from Mo(-II) to Mo(VI), but Mo (IV), Mo (V), Mo (VI) are the most important in the environment. Mo is present in most rocks and soils at levels between 1 and 10 mg/kg, and it is usually below 10 μg/L in most fresh waters [33]. However, under strongly reducing conditions the concentration of Mo in shale and mudstone can attain 100 mg/kg or higher [33]. Moreover, groundwater concentration can reach 25 mg/L near Mo ore districts [34]. Mo is used in additives, petroleum catalysts, plastics and fiber industries, corrosion inhibitors, and to control hardness in cast iron and stainless steel [35]. In agriculture it is used to supplement Mo deficiency in crops. The main human sources of Mo to the environment are industrial and agricultural pollution, and they include mobilization from

mine wastes, fuel (mostly coal) combustion and fly ash [36, 37]. Compared to other metals, Mo is toxicologically quite harmless and it usually does not have a serious health impact [34].

Commonly used Mo compounds are sulfides and oxides, and Mo oxides have more advantages than sulfides [38]. For example, nano molybdenum dioxide (MoO_2) particles have high stability, are easy to synthesize and can easily undergo surface modifications, which makes them interesting photothermal agents and carriers [39]. Further interesting features are low toxicity [40], low solubility [41], partial in-vivo degradability and rapid clearance [42]. Some scholars have studied the performance of nano MoO_2 in the field of catalysis. For example, Du et al. have studied MoO_2 as co-catalyst for hydrogen production, together with $Zn_{0.5}Cd_{0.5}S$ [43]. However, to our knowledge MoO_2 has never been studied in the field of AOPs.

In particular, the activation of PMS by nano MoO_2 has not been explored, and there are few reports on the AOP removal of naphthalene (a representative PAH) and its derivatives. Therefore, it is very meaningful to explore the degradation of PAHs by nano MoO_2/PMS.

In this study, naphthalene and some derivatives of environmental concern (1-methylnaphthalene, 1-nitronaphthalene, 1-chloronaphthalene, 1-naphthylamine, 1-naphthol) were selected as model contaminants, using nano MoO_2 as activator and PMS as oxidant. This work has the following goals: (a) Determination of the removal efficiency of contaminants with the nano MoO_2/PMS system, in the presence of different influencing factors. (b) Identification of the active species responsible for the degradation of the

pollutants. (c) Elucidation of the production and quenching processes of the reactive species in the nano MoO_2/PMS system. (d) Exploration of the effects of catalyst use, changes in use, and repeated use. (e) Elucidation of the transformation pathways of naphthalene and its derivatives under degradative conditions. The results of this study provide insight into a new technology for the degradation of PAHs and SPAHs, as well as an understanding of nano MoO_2 as new activator for the removal of organic contaminants from aqueous matrices.

2. Materials and Methods

2.1. Chemicals

Potassium peroxymonosulfate ($KHSO_5$, hereinafter PMS) was supplied by Shanghai Macklin Biochemical Corporation, Ltd (Shanghai, China). Naphthalene ($\geq 99.0\%$) and derivatives (1-methylnaphthalene, 1-nitronaphthalene, 1-chloronaphthalene, 1-naphthylamine, 1-naphthol) ($\geq 99.0\%$) were obtained from Sigma-Aldrich (Saint Louis, MO, USA). Nano molybdenum dioxide (Nano MoO_2, 99.9%) and nano molybdenum trioxide (Nano MoO_3, 99.95%) were purchased from Shanghai Maikun Chemical Corporation Ltd (Shanghai, China). 5,5-Dimethyl-1-pyrroline N-oxide (DMPO, 98%) and 2,2,6,6-tetramethylpiperidine (TEMP, $\geq 99\%$) were also supplied by Sigma-Aldrich (Saint Louis, MO, USA); tert-butyl alcohol (TBA), ethanol (EtOH), and $MoCl_5$ were purchased from Nanjing Chemical Reagent Corporation, Ltd (Nanjing, China). All water used was deionized, with a resistivity of 18.25 MΩ cm.

2.2. Degradation of naphthalene and derivatives by the nano MoO$_2$/PMS system

Batch experiments were performed in a shaker, using 40 mL EPA glass vials containing 20 mL reaction solution. Before each series of experiments, PMS stock solutions at concentrations of 10–240 mmol L^{-1} were prepared in ultrapure water, and a nano MoO$_2$ dosage of 0.05–0.5 g L^{-1} was also set to determine the effects of PMS concentration and nano MoO$_2$ dosage. The final nano MoO$_2$ dosage of (in most experiments) 0.05 g L^{-1} was obtained by dispersion of the solid into 19 mL of a solution containing a single compound chosen among naphthalene, 1-methylnaphthalene, 1-nitronaphthalene, 1-chloronaphthalene, 1-naphthylamine and 1-naphthol. After mixing, the solution pH (4.4–10.0) was adjusted with 1 mol L^{-1} H$_2$SO$_4$ or NaOH. Then, 1 mL of (usually) 80 mmol L^{-1} PMS stock solution was added to the system to start the reaction. The initial concentration of contaminants in the aqueous solution was 1 mg L^{-1}. The reaction solution with the appropriate MoO$_2$ loading was placed in a shaker to react at 200 r min^{-1} for 0–180 min. One mL of methanol was added to quench each 1 mL sample aliquot taken at intervals, and the residual contaminants were analyzed by high-performance liquid chromatography (HPLC). The PMS concentration was also determined, and the details are shown in the supporting information (SI). For electron paramagnetic resonance spectroscopy (EPR) analysis, aimed at the determination of free radicals, 1 mL DMPO (0.5 mol L^{-1}) or 1 mL TEMP (0.3 mol L^{-1}) was added to 5 mL of the nano MoO$_2$/PMS mixture and incubated for the designated time. All experiments were carried out in triplicate, and the data are here presented as the mean ± standard deviation (SD).

2.3. Analytical methods

The nano MoO_2 was analyzed directly using scanning electron microscopy (SEM; S-3400N II, Hitachi Limited, Japan) and transmission electron microscopy (TEM; JEM-2100, JEOL Corporation, Japan) to determine the surface structure. The analytical results are shown in Fig. S1. Phase analysis (Fig. S1) of nano MoO_2 was carried out by X-ray diffraction (XRD; X'TRA, ARL Company, Switzerland).

The sample/methanol mixture for liquid chromatography analysis was passed through a 0.22-μm filter, and then the residual naphthalene, 1-methylnaphthalene, 1-nitronaphthalene, 1-chloronaphthalene, 1-naphthylamine and 1-naphthol concentrations were determined using HPLC with a UV detector. To identify the intermediate degradation products, the reaction solution was extracted by methanol using solid-phase extraction with HLB packing. The extraction liquid was then concentrated under flowing nitrogen, and analyzed using liquid chromatography-mass spectrometry (LC-MS; Triple TOF 5600t MS, AB SCIEX, USA). Related details are provided in the SI.

Free radicals and $^1O_2$ in the nano MoO_2/PMS system were determined by EPR (Bruker Company, EMX-10/12, Germany); 0.1 mol L^{-1} DMPO and 0.03 mol L^{-1} TEMP were used as spin-trapping agents for, respectively, free radicals and $^1O_2$. The EPR spectra were recorded at room temperature using conditions of field center: 3480 G; sweep width: 200 G; static field: 3380 G; microwave frequency: 9.746 GHz; microwave power: 19.92 mW; receiver gain: 2.00×10^3; modulation frequency: 100.00 kHz; modulation amplitude: 1.00 G; time constant: 40.96; sweep time: 83.89 s. The relative concentrations of $SO_4^{\bullet-}$, $^\bullet OH$, $O_2^{\bullet-}$ and $^1O_2$ in the reaction solution were expressed as peak intensities signals of

DMPO-X and TEMP-$^1O_2$, with correction for the background noise.

To demonstrate the electron transfer mechanism, X-ray photoelectron spectroscopy (XPS, ESCALAB250Xi, Thermo Fisher Scientific, USA) was used to determine the chemical states of Mo in nano MoO_2.

The total concentration of leaching Mo ions in the nano MoO_2/PMS system was measured using inductively coupled plasma optical emission spectroscopy (ICP-OES, Optima 5300DV, Perkin Elmer, USA).

3. Results

3.1. Catalytic performances of nano MoO_2

The catalytic performance of the nano MoO_2/PMS system was investigated for the degradation and corresponding kinetic behavior of naphthalene and derivatives. Fig. 1 shows that almost no pollutants were removed by PMS alone in 180 min, meaning that PMS itself could hardly oxidize the studied contaminants. However, there was a major exception for 1-naphthylamine and (to a lesser extent) 1-naphthol. Indeed, 1-naphthylamine was degraded by 100% and 1-naphthol by 36% by PMS alone, without nano MoO_2 addition. Moreover, the studied pollutants were almost not consumed when nano MoO_2 alone was present, without PMS, with the only exception of naphthalene that was decreased by about 13%. Adsorption at the solid catalyst surface and/or volatilization are the most likely explanations for the limited disappearance of naphthalene in the presence of nano MoO_2 alone.

When nano MoO_2 and PMS occurred together, all the six contaminants underwent a sharp concentration drop, in agreement with the activation of PMS by the solid catalyst. In particular, the degradation percentage of naphthalene, 1-chloronaphthalene and 1-naphthylamine attained over 97% in 180 min (however, in the case of naphthylamine, the systems containing nano MoO_2 + PMS and PMS alone had very similar behavior). Moreover, 1-methylnaphthalene and 1-nitronaphthalene were degraded by more than 85%, while the degradation of 1-naphthol was slightly lower (around 77%). In several cases, degradation was almost complete within 40 minutes of the start of the reaction. A pseudo-first-order kinetic equation (SI) was used to fit the contaminants degradation curves (Fig. S2), and the pseudo-first-order rate constants k are listed in Fig. 1(g). Naphthalene and 1-chloronaphthalene had the highest degradation rate constants (respectively, 0.0700 and 0.0670 min^{-1}),followed by 1-methylnaphthalene, 1-nitronaphthalene, 1-naphthylamine and 1-naphthol (with respective rate constants of 0.0402, 0.0356, 0.0324 and 0.0242 min^{-1}). It is worth noting that 1-naphthylamine degraded about as fast in the presence of PMS alone (k = 0.0350 min^{-1}). In contrast, the degradation of 1-naphthol with PMS alone was significant (k = 0.0047 min^{-1}), but about 5-times slower compared to nano MoO_2 + PMS.

Moreover, it is shown in Fig. S3 that PMS was decomposed within the first 40 minutes from the start of the reaction. Its concentration then stabilized, which is consistent with the observed degradation kinetics of the contaminants.

3.2. Influence of pivotal factors

The loading of the activator (nano MoO_2 in the present case) is an important factor in

water treatment. Therefore, the effect of catalyst loading (0-0.5 g L^{-1}) on the removal of contaminants was investigated, and the results are shown in Fig. 2 panel A. As illustrated in Fig. 2(a)-(f), adding 0.05 g L^{-1} of nano MoO_2 could significantly improve the removal of most pollutants compared with the presence of PMS alone. Naphthalene could be completely degraded within 20 minutes when the loading of nano MoO_2 was increased to 0.1 g L^{-1}, and the degradation percentage of the other pollutants was also increased between 95% and 100% in the same conditions (except for 1-naphthol, for which the degradation approached 79%). When the loading of nano MoO_2 was further increased, all contaminants except 1-naphthol could be completely degraded in a short time. Therefore, the higher the loading of the activator, the higher was the degradation percentage of the pollutants, and the lesser was the time required for degradation. This observation holds in the case of 1-naphthylamine as well, for which nano MoO_2 accelerated the degradation significantly at loadings above 0.1 g L^{-1}. The associated pseudo-first order kinetic constants k were also obtained by data fitting (Fig. S4 panel A), and they are shown in Tab.1. The k values increased with increasing catalyst loading, except that in some cases at the highest loading (0.50 g L^{-1}) the reaction was too fast and could not be properly monitored. Therefore, it was not possible to apply a pseudo-first kinetic model to those experimental data.

The PMS concentration is directly related to the production of reactive oxygen species (ROS) [20]. Therefore, we also investigated the effect of PMS concentration, from 0 to 12 mmol L^{-1}, on the removal of naphthalene and its derivatives by nano MoO_2/PMS. The time trends are shown in Fig. 2 panel B, and the kinetic fit within 40 min is shown in Fig.

S4, panel B. As illustrated in Fig. 2(g)-(l), the concentration of PMS had positive but limited effect on the degradation of naphthalene and 1-chloronaphthalene. Because these two compounds already underwent effective degradation at low PMS, there was limited room for improvement with increasing PMS. In contrast, the degradation of both 1-nitronaphthalene and 1-naphthylamine was significantly improved as the concentration of PMS increased. In particular, 1-naphthylamine was completely degraded in 1 min with 12 mmol L^{-1} PMS, but in this casePMS alone had a key role in the process. The degradation of 1-methylnaphthalene and 1-naphthol was also increased with increasing PMS concentration, but complete degradation could not be reached even at the highest PMS levels. As shown in Tab. 1, the pseudo-first order k values of the six pollutants generally increased when increasing the PMS concentration. Moreover, the k values of naphthalene and 1-chloronaphthalene were usually higher than those of the other contaminants, except for 1-naphthylamine at high PMS (but here a peculiar process, not or poorly depending on MoO_2, was likely operational).

According to previous reports, the solution pH can affect the heterogeneous PMS oxidation systems by affecting the surface characteristics of the catalyst and the generation of radicals [44-47]. Fig. 2 panel C and Fig. S4 panel C report the degradation trends of naphthalene and its derivatives at different pH values. The degradation percentages of naphthalene, 1-methylnaphthalene, 1-nitronaphthalene and 1-chloronaphthalene decreased significantly with increasing pH from 4.4 to 10.0, and the k values were correspondingly reduced. The pH effect was particularly evident in the case of 1-nitronaphthalene. As far as 1-naphthol is concerned, its initial degradation kinetics was slowed down by the pH

increase, but the degradation percentage at 180 min varied very little with pH. In contrast, 1-naphthylamine was the only contaminant for which the degradation became both faster and more efficient with increasing pH.

3.3. Identification of reactive species in the nano MoO$_2$/PMS system

The activation of PMS usually yields free radicals such as $SO_4^{\bullet-}$, $^{\bullet}OH$ and $O_2^{\bullet-}$. In addition, singlet oxygen ($^1O_2$) and non-radical processes also contribute to the degradation of contaminants [48, 49]. We studied the degradation mechanism of naphthalene and its derivatives in the nano MoO$_2$/PMS system by identifying a series of free radical species and $^1O_2$, and by carrying out quenching experiments. EPR analysis, combined with DMPO and TEMP as spintronic capture agents, was used to determine the presence of these active species. As shown in Fig. 3, the free radical capture signals DMPO-$SO_4^{\bullet-}$ (hyperfine coupling constants of $\alpha_N = 13.2$ G, $\alpha_H = 9.6$ G, $\alpha_H = 1.48$ G, and $\alpha_H = 0.78$ G) and DMPO-$^{\bullet}OH$ (hyperfine coupling constants of $\alpha_N = \alpha_H = 14.9$ G) were clearly visible at 1-10 min in all the six degradation systems [50]. Moreover, Fig. S5(a) shows that PMS alone did not produce any free radicals, the occurrence of which is thus accounted for by the activation of PMS by nano MoO$_2$. Among the detected radicals, $SO_4^{\bullet-}$ gradually decreased along with the increase of $^{\bullet}OH$, and the peak intensity of DMPO-$^{\bullet}OH$ was significantly higher compared to that of DMPO-$SO_4^{\bullet-}$.

In order to further distinguish the contribution of the two species in the degradation of the six studied pollutants, we used the chemical quenchers ethanol (EtOH, $k(\text{EtOH}+SO_4^{\bullet-})$ = $(1.6 - 7.7) \times 10^7$ M^{-1}s^{-1}; $k(\text{EtOH}+^{\bullet}OH) = (1.2 - 2.8) \times 10^9$ M^{-1}s^{-1}) and tert-butanol (TBA, $k(\text{TBA}+SO_4^{\bullet-}) = (4.0 - 9.1) \times 10^5$ M^{-1}s^{-1}; $k(\text{TBA}+^{\bullet}OH) = (3.8 - 7.6) \times 10^8$ M^{-1}s^{-1}) [51, 52].

As illustrated in Fig. 4, the quenching experiments were carried out with concentration ratios of EtOH(TBA)/PMS = 200 and 500. Both EtOH and TBA were able to significantly quench the degradation of naphthalene, 1-methylnaphthalene, 1-nitronaphthalene and 1-chloronaphthalene. In contrast, as shown in Fig. 4(e,f), the quenchers had a much smaller effect on the degradation of 1-naphthylamine and 1-naphthol. Interestingly, these are the same compounds that could be degraded by PMS alone.

Other active species occurring in the nano MoO$_2$/PMS system were also detected by EPR with DMPO as electron spin trap, where the signal of DMPO-OOH (combination of O$_2^{\bullet-}$ and DMPO) was very obvious as shown in Fig. 5(a). O$_2^{\bullet-}$ was not found in the presence of PMS alone (Fig. S5(b)). The production of ^{1}O$_2$ in the six systems was studied with TEMP as a capture agent, and the results are shown in Fig 5(b). An obvious TEMP-^{1}O$_2$ signal peak was found here. The TEMP-^{1}O$_2$ signal peak also appeared when TEMP was alone (see Fig. S5 (c)). This is because TEMP was oxidized, but the peak height in the presence of MoO$_2$/PMS was significantly enhanced, so ^{1}O$_2$ was generated in this system. The two species O$_2^{\bullet-}$ (-0.33 V) and ^{1}O$_2$ are rather weak oxidants, thus their ability to induce pollutant degradation may be limited. The scavenging experiments with EtOH and TBA suggest that SO$_4^{\bullet-}$ and $^{\bullet}$OH largely predominate in the degradation of naphthalene, 1-methylnaphthalene, 1-nitronaphthalene and 1-chloronaphthalene (in the presence of EtOH or TBA in excess, the degradation of these compounds was practically negligible). The degradation of 1-naphthylamine can be accounted for by reaction with PMS, thereby excluding an important role of other reactive species. In the case of 1-napthol the inhibition of degradation by the alcohols was not complete, thus there is

potential for reactive species other than $SO_4^{\bullet-}$ and $^{\bullet}OH$ to take part to degradation. However, possible secondary reactions induced by, e.g., alcohol-derived radicals should be taken into account before invoking a role of additional reactive species such as $O_2^{\bullet-}$ and $^1O_2$ (*vide infra*, section 4.3, for a discussion over this issue).

3.4. Surface investigation and stability of the nano MoO_2

It is well known that PMS activation by metals occurs because the O-O bond in the PMS molecule ($HO\text{-}SO_4^-$) is homolytically cleaved to produce $SO_4^{\bullet-}$ upon acceptance of one electron from the transition metal [53]. Therefore, the role of nano MoO_2 in PMS activation is worth exploring. The surface changes in the catalyst were investigated by XPS, and the results are shown in Fig. 6. The wide XPS spectrum of the sample shows that the catalyst includes C, O, and Mo. We can easily see six distinct peaks, two of which are C 1s and O 1s with peaks centered at 284.08 eV and 530.08 eV. The other four peaks are Mo 4p, Mo 3d, Mo 3p3/2, and Mo 3p1/2, with binding energies of 38.08, 232.08, 396.08 and 413.08 eV, respectively. The Mo 3d high–resolution peak could be deconvoluted into six peaks, as shown in Fig 6 (A)–(F). The corresponding binding energies are listed in detail in Tab. S1. The strong deconvoluted peaks with binding energies of 228.87 and 232.04 eV are Mo (VI) double peaks corresponding to Mo 3d5/2 and Mo 3d3/2 in nano MoO_2, respectively [54]. We also found that the deconvoluted peak of Mo (V) and Mo (IV) in the nano MoO_2 sample after the reaction showed a binding energy of, respectively, 230.20 eV (Mo 3d5/2) and 233.86 eV (Mo 3d3/2), and of 231.38 eV (Mo 3d5/2) and 235.00 eV (Mo 3d3/2) [54]. Moreover, the XPS spectra of nano MoO_2 in the six pollutant degradation systems were almost the same, presumably because the

modifications of nano MoO_2 are due to the interaction with PMS and not with the pollutants.

We also measured the leaching of ionic Mo at different pH values in the degradation systems. As illustrated in Fig. S7(a) the leaching amount of Mo ions was not much different for the studied pollutants, and it was in the range of 15-20 mg L^{-1}. Mo leaching decreased with increasing pH, with the only exception of the system containing 1-naphthylamine.

The following step was to check whether leached Mo could activate PMS and induce the degradation of the contaminants. We carried out these homogeneous-phase activation experiments using 1 mmol L^{-1} Mo(V) ions, because the commercial Mo(IV) compounds are poorly water-soluble. As shown in Fig. S7(b), the homogeneous Mo(V)/PMS system was able to induce the degradation of all the studied contaminants, with the best degradations observed for naphthalene, 1-methylnaphthalene and especially 1-naphthol, and the worst for 1-naphthylamine. These findings suggest that leached Mo(V) could play a significant a role in the degradation of contaminants by nano MoO_2/PMS.

The stability of nano MoO_2 was examined by collecting and reusing it in four cycles, with results shown in Tab. 2. The removal of the contaminants in the second and third use of nano MoO_2 had gradually deteriorated, except for 1-naphthylamine that could be degraded by PMS alone. However, when using nano MoO_2 for the fourth time, the degradation rate of the five pollutants (with the usual exception of 1-naphthylamine, for which nothing changed) was significantly improved compared to the second and third stages.

3.5. Degradation intermediates and pathways of naphthalene and derivatives

During the degradation of the studied contaminants in the nano MoO_2/PMS system, several intermediates were identified by LC-MS. In particular, we found 10 intermediates formed from naphthalene, 13 from 1-methylnaphthalene, 4 from 1-nitronaphthalene, 13 from 1-chloronaphthalene, 12 from 1-naphthylamine, and 10 from 1-naphthol. Detailed MS spectra of the mentioned intermediates are reported in Fig. S8-S69, and there were common products between the contaminants. Based on the detected intermediates and previously reported results [55-62], we propose some degradation pathways for each contaminant as shown in Fig. 7. To account for the formation of the positively detected intermediates we had to speculate about the possible formation of non-detected compounds (presumably escaping detection because of low stability in the studied systems), which would act as precursors through known transformation pathways. These compounds are square-bracketed in the figure panels.

Naphthalene (Fig. 7(a)) first yielded naphthol (A,H) by hydroxylation [61], then probably the hydroxyl group was substituted by a methyl group to produce a methylnaphthalene. We propose the formation of this compound, although it was not directly detected, because its oxidation could then yield 4-hydroxy-4-methylnaphthalen-1(4H)-one (B). This and other transformation processes proceeded through C-atom addition, suggesting that oxidation/fragmentation pathways likely yielded carbon-based radicals in addition to the transient species identified by EPR [55, 59]. Secondly, hydroxynaphthalene was carbonylated to form 4-hydroxy-1-naphthoic acid (D), or further degraded by oxidation and/or ring opening to produce o-phthalic

anhydride (E), phthalic acid (F), acetophenone (K), 4-hydroxy-1,2-naphoquinone (L), 2-hydroxycinnamic acid (N) and 2-hydroxy-1-naphthoic acid (M) [58, 61].

The degradation pathway of 1-methylnaphthalene is shown in Fig. 7(b). Similarly to naphthalene also this compound underwent hydroxylation, and then the aromatic ring was oxidatively attacked to produce 4-hydroxy-4-methylnaphthalen-1(4H)-one (B). Another route was the oxidation of the methyl functional group to produce 1-naphthaldehyde (O) [55]. Oxidative decarboxylation would then form naphthalene (R), which can undergo hydroxylation as per the pathway described before. In addition, ring contraction and hydroxylation processes can yield hydroquinone (P). The occurrence of reducing transient species such as $O_2^{\bullet-}$ in the reaction system can account for reduction pathways, such as the transformation of 1,2-dihydroxynaphthalene (I) into 1,2-dihydro-1,2-dihydroxynaphthalene (S) [59].

The degradation pathway of 1-nitronaphthalene is shown in Fig. 7(c), and it is relatively simple compared to the other contaminants under study. Because nitronaphthalene shares several transformation intermediates with naphthylamine (*vide infra*), we speculate that its transformation also involves reduction to 1-naphthylamine, although the latter was not detected (note that the degradation of 1-naphthylamine was typically faster compared to 1-nitronaphthalene). Indeed, from 1-naphthylamine it is easy to hypothesize hydroxylative substitution followed by oxidative ring opening, to form o-phthalic anhydride (E) and carboxyl cinnamaldehydes (J). Moreover, hydroxylation at the *ortho* and *para* positions of the nitro functional group would yield 1-nitro-1,2-dihydronaphthalen-2-ol (T) and 4-hydroxy-1-nitronaphthalene (U).

The degradation pathway of 1-chloronaphthalene is shown Fig. 7(d), and it bears similarities with the transformation of naphthalene. The chlorine atom was hydroxyl-substituted to form hydroxynaphthalene (A), which then underwent carbonylation and further oxidative degradation. As shown above, 1,2-dihydroxynaphthalene (I) can be hydrogenated to form 1,2-dihydro-1,2-dihydroxynaphthalene (S). In addition, the para position of 1-chloronaphthalene was hydroxylated to form 4-chloronaphthalen-1-ol (V), further hydroxylated to 4-chloronaphthalene-1,2-diol (W), and finally oxidized to (E)-2-(1-chloro-3-oxoprop-1-en-1-yl)benzaldehyde (X) [56]. Moreover, the naphthalene ring could be attacked, oxygenated, opened, and oxidatively degraded to form 2-formylbenzoyl chloride (Y) [56].

The degradation pathway of 1-naphthylamine is shown in Fig. 7(e). The loss of the nitrogen atom in some intermediates leads us to speculate that substitution-hydroxylation might have yielded naphthol (not directly detected) [57], which could undergo oxidation/ring fragmentation to produce 2-hydroxycinnamic acid (N) and then (2Z,4Z)-hexa-2,4-dienedioic acid (e). Other conversion processes for naphthol are similar to naphthalene, as described above. A parallel reduction process (possibly to naphthalene) followed by ring contraction could yield indene (b), which could be degraded to 2-butyl-1,4-dimethylbenzene (c) by methyl substitution and ring opening [59]. Naphthalene would also be a candidate substrate to undergo methylation and then oxidation of the methyl functional group to produce 1-naphthylmethanol (d) [55]. A further degradation pathway involved the amino functional group of 1-naphthylamine,

which was oxidatively converted to 1-nitrosonaphthalene (f) and then to 1-nitronaphthalene (g). The nitroderivative was then hydroxylated to produce 1-nitro-1,2-dihydronaphthalen-2-ol (T).

The degradation pathway of 1-naphthol is reported Fig. 7(f). Part of the degradation process is similar to that undergone by 1-naphthol as an intermediate of naphthalene degradation. In addition, 1-naphthol was involved in ring contraction and then ring opening, chain scission and hydroxylation to finally produce hydroquinone (P) [59]. Another reaction pathway involving ring fragmentation would produce tetramethylbenzene (h) [59]. Furthermore, 1-naphthol underwent methylation followed by oxidation of the methyl functional group, to give 1-naphthylmethanol (d) [55].

4. Discussion

4.1. Nano MoO$_2$ performed well in the catalytic degradation of naphthalene and derivatives

Our results show that nano MoO$_2$ can activate PMS, and both components are required in most cases for degradation to proceed properly. Nano MoO$_2$ alone gives little contribution to the degradation of pollutants, but 1-naphthylamine and 1-naphthol were degraded in the presence of PMS alone that has weak oxidative properties [63]. For instance, PMS alone has shown some potential to degrade Bisphenol F [23]. Activation of PMS by nano MoO$_2$ is further demonstrated by the concentration decrease of PMS itself with the reaction time.

4.2. Pivotal factors that affected the generation and occurrence of reactive species

Degradation was usually favored by an increase in PMS concentration or nano MoO_2 loading, which would both enhance the production of reactive transient species. An increase in the loading of nano MoO_2 would in fact provide more available active sites, accelerating the activation of PMS on the catalyst surface and producing a large amount of ROS, which trigger the degradation of naphthalene and its derivatives [20]. Similarly, by increasing the PMS concentration one would also enhance ROS production by better exploiting the nano MoO_2 active sites [64]. Moreover, increasing PMS would favor the degradation of 1-naphthylamine and 1-naphthol, even in the absence of nano MoO_2.

With the exception of 1-naphthylamine, increasing pH was usually detrimental to degradation by nano MoO_2/PMS. A possible explanation for this finding is the fact that PMS ($pK_{a1}=0$, $pK_{a2}=9.4$ [65]) undergoes acid-base equilibria, with the form HSO_5^- prevailing at acidic pH. Therefore, our hypothesis is that HSO_5^- is easier to be activated by nano MoO_2 compared to SO_5^{2-}, which prevails at pH 10 [66]. Another possibility is the enhanced decomposition of HSO_5^- at basic pH, which would inhibit degradation [67]:

$$2\ HSO_5^- + 2OH^- \rightarrow 2SO_4^{2-} + O_2 + 2\ H_2O \tag{1}$$

Basic conditions can also enhance the interconversion of $SO_4^{\bullet-}$ into $^{\bullet}OH$ [68]:

$$SO_4^{\bullet-} + OH^- \rightarrow SO_4^{2-} + {}^{\bullet}OH \qquad k = 7.3\times10^7\ M^{-1}s^{-1} \tag{2}$$
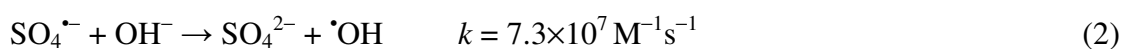
In neutral and basic solutions the redox potential of $^{\bullet}OH$ is lower than that of $SO_4^{\bullet-}$ [69], but in many cases the reaction rate constants of the two radicals with the pollutants are not very different in any pH condition (and often, $^{\bullet}OH$ is more reactive than $SO_4^{\bullet-}$ despite the lower redox potential) [69, 70].

Differently from the other pollutants, increasing pH enhanced the degradation of 1-naphthylamine. This compound undergoes degradation by PMS alone, thus two possible explanations can account for the pH effect: *(i)* the degradation of 1-naphtylamine occurs to a higher extent upon reaction with SO_5^{2-}, which prevails under basic conditions, and/or *(ii)* degradation is more difficult in the presence of the protonated substrate (1-naphthylammonium) in acidic conditions.

4.3. Reactive species that played an important role in degradation of naphthalene and its derivatives

The spin-trapping experiments indicated that both $^{\bullet}OH$ and $SO_4^{\bullet-}$ occurred in the nano MoO_2/PMS system. Indeed, the generated $SO_4^{\bullet-}$ can be quickly converted into $^{\bullet}OH$ in aqueous solution, according to Eqs. (2) and (3) [71, 72].

$$SO_4^{\bullet-} + H_2O \rightarrow SO_4^{2-} + {}^{\bullet}OH + H^+ \tag{3}$$

The quenching experiments with the alcohols also indicated that both $^{\bullet}OH$ and $SO_4^{\bullet-}$ would play key roles in the degradation of naphthalene, 1-methylnaphtalene, 1-nitronaphthalene and 1-chloronaphthalene. In contrast, the added alcohols were much less effective to inhibit the degradation of either 1-naphthylamine or 1-naphthol. In the former case the limited inhibition is due to the fact that 1-naphthylamine is degraded by PMS alone, thus the activation of PMS by nano MoO_2 is not necessary for degradation. The same explanation hardly applies to 1-naphthol, because degradation was faster and more extensive with nano MoO_2/PMS compared to PMS alone. However, the added alcohols would produce secondary radical species upon reaction with $^{\bullet}OH/SO_4^{\bullet-}$, and the effect of these species should be considered. For this reason, the production of free

radicals was determined as well in the nano MoO_2/PMS/EtOH and the nano MoO_2/PMS/TBA systems. As shown in Fig. S70(a), the alcohol radicals $^{\bullet}CH_2CH_2OH$ were formed in the nano MoO_2/PMS/EtOH system. These and similar radicals have strong reducing ability (reduction potentials ranging from -1.39V to -1.18V), which could enable them to degrade pollutants [73, 74]. For instance, Fang et al. have reported that TBA radicals reductively degraded PCBs that are otherwise difficult to degrade. Fig. S70(b) shows the signals relative to trapped $SO_4^{\bullet-}$ and $^{\bullet}OH$ at 10 min in the nano MoO_2/PMS/TBA system. Compared to the system without alcohol, only $^{\bullet}OH$ was significantly reduced. This result is consistent with the TBA reaction rate constants with $SO_4^{\bullet-}$ and $^{\bullet}OH$ [69, 70], and suggests that TBA scavenges $^{\bullet}OH$ to a higher extent than $SO_4^{\bullet-}$. The fact that TBA did not affect the degradation of 1-naphthol (while, for comparison, EtOH slightly inhibited it, see Fig. 4(f)) suggests that 1-naphthol might be mainly degraded by reaction with $SO_4^{\bullet-}$ in the nano MoO_2/PMS system.
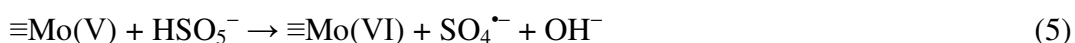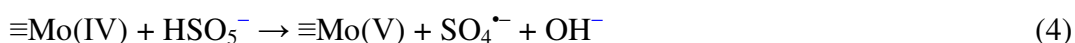
The EPR spectra of $O_2^{\bullet-}$ and $^1O_2$ indicated that both free radicals occurred in the nano MoO_2/PMS system. However, the quenching experiments with EtOH and TBA suggest that reactive species different from $^{\bullet}OH$ and $SO_4^{\bullet-}$ are little likely to be involved significantly in the degradation of naphthalene, 1-methylnaphthalene, 1-nitronaphthalene, and 1-chloronaphthalene. The degradation of 1-naphthylamine is well accounted for by PMS alone, while in the case of 1-naphthol the alcohols were unable to fully quench degradation. However, the effect of the alcohols on 1-naphthol could be accounted for in the hypothesis that $SO_4^{\bullet-}$ were the main reactive species and that EtOH produced reactive secondary radicals. Therefore, a significant involvement of $O_2^{\bullet-}$ and $^1O_2$ in the degradation

of 1-naphthol cannot be conclusively demonstrated.

4.4. Catalytic mechanism

The double peaks of Mo(V) and Mo(VI) appearing in the XPS spectra of the reacted nano MoO_2 can be accounted for by oxidation reactions on the surface of nano MoO_2 [76]. Mo(IV) activates PMS by transferring one or two electrons, and undergoing transformation into Mo(V) and Mo(VI) according to the Eqs. (4) - (5):

$$\equiv Mo(IV) + HSO_5^- \rightarrow \equiv Mo(V) + SO_4^{\bullet-} + OH^- \qquad (4)$$

$$\equiv Mo(V) + HSO_5^- \rightarrow \equiv Mo(VI) + SO_4^{\bullet-} + OH^- \qquad (5)$$

This process is depicted in Fig. 9. A similar activation process was also described in other systems that use transition metals oxides, such as Fe_2O_3 and V_2O_3 as catalysts [44, 77].
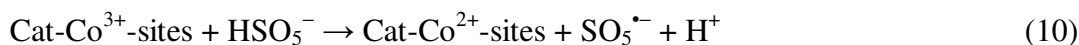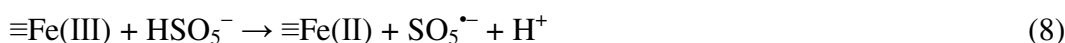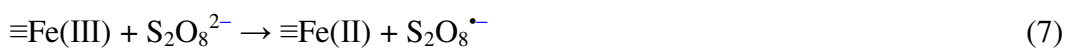
The observed leaching of Mo ions in nano MoO_2/PMS and the activation experiments with Mo(V)/PMS suggest that homogeneous and heterogeneous catalysis may both occur in the nano MoO_2/PMS system. The activation of PMS by Mo(V) could take place as shown in Eq. (6):
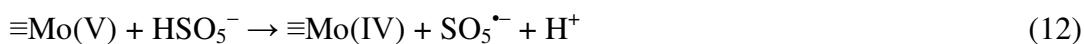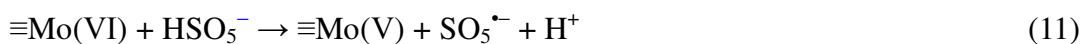
$$Mo(V) + HSO_5^- \rightarrow Mo(VI) + SO_4^{\bullet-} + OH^- \qquad (6)$$
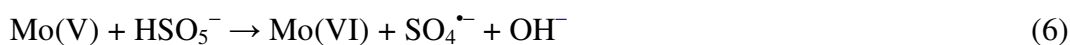
The pH of the solution after the homogeneous reaction was about 2.3, which is not conducive to the conversion of $SO_4^{\bullet-}$ into $^{\bullet}OH$. Interestingly and coherently, the homogeneous system was particularly effective in the degradation of 1-naphthol (see Fig. S7(b)), for which there is independent evidence that degradation mainly involved $SO_4^{\bullet-}$.

The oxidation of the surface Mo(IV) groups can account for the decrease of the activity of nano MoO_2 when it is reused several times. However, differently from typical

findings where catalytic effects are either unchanged or gradually deteriorate with use [78, 79], we showed here that the activity was partially recovered from the 3rd to the 4th reuse. We can speculate that the regeneration of ≡Mo(IV) or ≡Mo(V) on the surface of nano MoO$_2$ particles, upon reduction of ≡Mo(VI), might be a possible factor influencing the catalytic activity. Some researchers have activated persulfate or PMS with iron, vanadium oxides and composite catalyst, finding a similar reduction process according to Eqs. (7) - (10) [53, 77, 80, 81].

$$\equiv Fe(III) + S_2O_8{}^{2-} \rightarrow \equiv Fe(II) + S_2O_8{}^{\bullet-} \tag{7}$$

$$\equiv Fe(III) + HSO_5{}^{-} \rightarrow \equiv Fe(II) + SO_5{}^{\bullet-} + H^+ \tag{8}$$

$$\equiv V(V) + S_2O_8{}^{2-} \rightarrow \equiv V(IV) + S_2O_8{}^{\bullet-} \tag{9}$$

$$Cat\text{-}Co^{3+}\text{-sites} + HSO_5{}^{-} \rightarrow Cat\text{-}Co^{2+}\text{-sites} + SO_5{}^{\bullet-} + H^+ \tag{10}$$

We hypothesize that, in the presence of excess ≡Mo(VI) on the catalyst surface, a reduction process can be triggered according to Eqs. (11) - (12), and the ≡Mo(IV) formed upon reduction could activate again PMS. At the same time, these processes would produce SO$_5{}^{\bullet-}$ that has weak oxidizing ability (E(SO$_5{}^{\bullet-}$) = 1.1 V) and could be involved as well in the degradation of pollutants [53].

$$\equiv Mo(VI) + HSO_5{}^{-} \rightarrow \equiv Mo(V) + SO_5{}^{\bullet-} + H^+ \tag{11}$$

$$\equiv Mo(V) + HSO_5{}^{-} \rightarrow \equiv Mo(IV) + SO_5{}^{\bullet-} + H^+ \tag{12}$$

In order to verify this hypothesis we carried out degradation experiments with nano MoO$_3$ as activator, and the results are shown in Fig. S71. The six pollutants show different degrees of degradation in the nano MoO$_3$/PMS system (naphthalene 23%, 1-methylnaphthalene 21%, 1-nitronaphthalene 5%, 1-chloronaphthalene 33%,

1-naphthylamine 100% and 1-naphthol 100%). It should be remarked that the complete degradation of 1-naphthylamine was mainly due to the oxidative properties of PMS itself. On the other hand, the complete degradation of 1-naphthol can be accounted for by the activation of PMS by nano MoO$_3$. Furthermore, we also found by EPR a weak $^\bullet$OH signal (Fig. S72) in the nano MoO$_3$/PMS system. This could be due to the formation of SO$_4^{\bullet-}$ upon reduction of Mn(VI) to Mn(IV) and activation of PMS by Mn(IV). The radical SO$_4^{\bullet-}$ would then trigger the oxidation of H$_2$O/OH$^-$ to $^\bullet$OH.

Based on the above findings, we can postulate the activation mechanism of nano MoO$_2$ on PMS as shown in Fig. 9. Finally, a further minor process might partially account for the (limited) degradation of 1-naphthol in the presence of nano MoO$_2$ alone. Indeed, the interaction between 1-naphtol and nano MoO$_2$ produced carbon-centered environmentally persistent free radicals (EPFRs) (Fig. S73(a)), presumably via physicochemical adsorption and electron transfer (the postulated formation process is shown in Fig. S73(b)). There are many reports on the formation of EPFRs [82, 83], and it is also reported that they could activate PS or PMS [84, 85]. This will be the topic of forthcoming research.

4.5. Common degradation pathways between some of the studied contaminants

According to the results of the degradation pathways of the six pollutants, 1-naphthol was a common transformation intermediate in at least some cases. This compound could be formed by hydroxylation of naphthalene, or by substitution/hydroxylation in the other cases. 1-Naphthol was then degraded to o-phthalic anhydride and carboxyl cinnamaldehydes by hydroxylation and oxidative degradation. Another common pathway

between naphthalene, 1-methylnaphthalene, 1-chloronaphthalene, 1-naphthylamine and 1-naphthol would be the conversion of 1-naphthol to 4-hydroxy-1-naphthoic acid, by hydroxylation and carbonylation. The interconversion between naphthalene pollutants has also been described in previous reports [57, 59, 61].

In the case of substituted naphthalenes, oxidative (or reductive) transformation could involve either the functional group or the aromatic ring (the reductive pathway, possibly involving $O_2^{\bullet-}$, was for instance operational in the transformation of -NO_2 into -NH_2).

5. Conclusion

Nano MoO_2 is a promising catalyst for the activation of PMS, in the framework of the degradation of naphthalene and its derivatives, owing to its high catalytic efficiency and potential reusability. Here we have shown that nano MoO_2 can activate PMS by electron transfer, producing $SO_4^{\bullet-}$ and later $^{\bullet}OH$ upon reaction of $SO_4^{\bullet-}$ with water and OH^-. The two radical species are involved in the degradation of most of the studied pollutants, except for 1-naphthylamine that was degraded by reaction with PMS alone. Moreover, 1-naphthol mainly underwent degradation by reaction with $SO_4^{\bullet-}$. Spin-trapping experiments suggested that additional transient species ($O_2^{\bullet-}$ and $^1O_2$) were formed in the system but depending on the substrate, a key role of these species in the degradation of contaminants is either excluded or not clearly apparent. Part of the degradation process triggered by nano MoO_2 is likely accounted for by the leaching of Mo ions, which can activate PMS by means of homogeneous-phase reactions. The surface of MoO_2 is oxidized during PMS activation, and this process can account for the loss in activity as the catalyst

is reused. However, the formation of high-valence surface species (Mo(VI)) detected by XPS spectroscopy might be the basis for the partial restoration of the catalytic activity in further reuse cycles, because Mo(VI) could be reduced back to Mo(IV) that activates PMS. In summary, this study provides a new way to efficiently activate PMS with a new catalyst that can be used in advanced oxidation processes.

Appendix A. Supplementary data

Supplementary data associated with this article can be found, in the online version, at https://???

References

[1] M. Usman, P. Faure, C. Ruby, K. Hanna, Remediation of PAH-contaminated soils by magnetite catalyzed Fenton-like oxidation, Applied Catalysis B: Environmental, 117-118 (2012) 10-17.

[2] J. Zhang, L. Yang, F. Ledoux, D. Courcot, A. Mellouki, Y. Gao, P. Jiang, Y. Li, W. Wang, PM2.5-bound polycyclic aromatic hydrocarbons (PAHs) and nitrated PAHs (NPAHs) in rural and suburban areas in Shandong and Henan Provinces during the 2016 Chinese New Year's holiday, Environmental Pollution, 250 (2019) 782-791.

[3] M.M.R. Mostert, G.A. Ayoko, S. Kokot, Application of chemometrics to analysis of soil pollutants, TrAC Trends in Analytical Chemistry, 29 (2010) 430-445.

[4] I. Adánez-Rubio, F. Viteri, Á. Millera, R. Bilbao, M.U. Alzueta, S-PAH, oxy-PAH and EPA-PAH formation during ethylene-SO2 pyrolysis, Fuel Processing Technology, 182 (2018) 68-76.

[5] L. Chu, S. Yu, J. Wang, Gamma radiolytic degradation of naphthalene in aqueous solution, Radiation Physics and Chemistry, 123 (2016) 97-102.

[6] M. Masuda, Q. Wang, M. Tokumura, Y. Miyake, T. Amagai, Simultaneous determination of polycyclic aromatic hydrocarbons and their chlorinated derivatives in grilled foods, Ecotoxicology and Environmental Safety, 178 (2019) 188-194.

[7] Y. Kojima, K. Inazu, Y. Hisamatsu, H. Okochi, T. Baba, T. Nagoya, Influence of secondary formation on atmospheric occurrences of oxygenated polycyclic aromatic hydrocarbons in airborne particles, Atmospheric Environment, 44 (2010) 2873-2880.

[8] M. Qiao, W. Qi, H. Liu, Y. Bai, J. Qu, Formation of oxygenated polycyclic aromatic hydrocarbons from polycyclic aromatic hydrocarbons during aerobic activated sludge treatment and their removal process, Chemical Engineering Journal, 302 (2016) 50-57.

[9] M. Qiao, L. Fu, Z. Li, D. Liu, Y. Bai, X. Zhao, Distribution and ecological risk of substituted and parent polycyclic aromatic hydrocarbons in surface waters of the Bai, Chao, and Chaobai rivers in northern China, Environmental Pollution, (2019) 113600.

[10] A.D. Sekar, H. Muthukumar, N.I. Chandrasekaran, M. Matheswaran, Photocatalytic degradation of naphthalene using calcined FeZnO/ PVA nanofibers, Chemosphere, 205 (2018) 610-617.

[11] Y. Chen, G. Sheng, X. Bi, Y. Feng, B. Mai, J. Fu, Emission Factors for Carbonaceous Particles and Polycyclic Aromatic Hydrocarbons from Residential Coal Combustion in China, Environmental Science & Technology, 39 (2005) 1861-1867.

[12] J. Lewtas, Air pollution combustion emissions: Characterization of causative agents and mechanisms associated with cancer, reproductive, and cardiovascular effects, Mutation Research/Reviews in Mutation Research, 636 (2007) 95-133.

[13] T. Nielsen, Reactivity of polycyclic aromatic hydrocarbons towards nitrating species, Environmental Science & Technology, 18 (1984) 157-163.

[14] R. Atkinson, J. Arey, Atmospheric chemistry of gas-phase polycyclic aromatic hydrocarbons: formation of atmospheric mutagens, Environmental Health Perspectives, 102 (1994) 117-126.

[15] J. Zhan, Y. Yang, D. Liu, Y. Sun, H. Li, W. Wang, Research progress on nitro polycyclic aromatic hydrocarbons in the atmosphere, Science in China: Earth Sciences, 42 (2012) 1-9.

[16] I. Espadaler, E. Eljarrat, J. Caixach, J. Rivera, I. Martí, F. Ventura, Assessment of Polychlorinated Naphthalenes in Aquifer Samples for Drinking Water Purposes, Rapid Communications in Mass Spectrometry, 11 (1997) 410-414.

[17] I. Martí, F. Ventura, Polychlorinated naphthalenes in groundwater samples from the Llobregat aquifer (Spain), Journal of Chromatography A, 786 (1997) 135-144.

[18] L.C. Erickson Md Fau - Michael, R.A. Michael Lc Fau - Zweidinger, E.D. Zweidinger Ra Fau - Pellizzari, E.D. Pellizzari, Sampling and analysis for polychlorinated naphthalenes in the environment.

[19] J. Hu, D. Shao, C. Chen, G. Sheng, X. Ren, X. Wang, Removal of 1-naphthylamine from aqueous solution by multiwall carbon nanotubes/iron oxides/cyclodextrin composite, Journal of Hazardous Materials, 185 (2011) 463-471.

[20] P. Sun, H. Liu, M. Feng, L. Guo, Z. Zhai, Y. Fang, X. Zhang, V.K. Sharma, Nitrogen-sulfur co-doped industrial graphene as an efficient peroxymonosulfate activator: Singlet oxygen-dominated catalytic degradation of organic contaminants, Applied Catalysis B: Environmental, 251 (2019) 335-345.

[21] M. Boulangé, C. Lorgeoux, C. Biache, A. Saada, P. Faure, Fenton-like and potassium

permanganate oxidations of PAH-contaminated soils: Impact of oxidant doses on PAH and polar PAC (polycyclic aromatic compound) behavior, Chemosphere, 224 (2019) 437-444.

[22] X. Chen, B. Yang, P. Oleszczuk, Y. Gao, X. Yuan, W. Ling, M.G. Waigi, Vanadium oxide activates persulfate for degradation of polycyclic aromatic hydrocarbons in aqueous system, Chemical Engineering Journal, 364 (2019) 79-88.

[23] S.B. Hammouda, F. Zhao, Z. Safaei, D.L. Ramasamy, B. Doshi, M. Sillanpää, Sulfate radical-mediated degradation and mineralization of bisphenol F in neutral medium by the novel magnetic Sr2CoFeO6 double perovskite oxide catalyzed peroxymonosulfate: Influence of co-existing chemicals and UV irradiation, Applied Catalysis B: Environmental, 233 (2018) 99-111.

[24] D. Liu, M. Li, X. Li, F. Ren, P. Sun, L. Zhou, Core-shell Zn/Co MOFs derived Co3O4/CNTs as an efficient magnetic heterogeneous catalyst for persulfate activation and oxytetracycline degradation, Chemical Engineering Journal, (2020) 124008.

[25] G.P. Anipsitakis, D.D. Dionysiou, Transition metal/UV-based advanced oxidation technologies for water decontamination, Applied Catalysis B-Environmental, 54 (2004) 155-163.

[26] F. Yang, B. Sheng, Z. Wang, R. Yuan, Y. Xue, X. Wang, Q. Liu, J. Liu, An often-overestimated adverse effect of halides in heat/persulfate-based degradation of wastewater contaminants, Environment International, 130 (2019) 104918.

[27] M.-Y. Lee, W.-L. Wang, Z.-B. Xu, B. Ye, Q.-Y. Wu, H.-Y. Hu, The application of UV/PS oxidation for removal of a quaternary ammonium compound of dodecyl trimethyl ammonium chloride (DTAC): The kinetics and mechanism, Science of The Total Environment, 655 (2019) 1261-1269.

[28] L.A. Achola, A. Ghebrehiwet, J. Macharia, P. Kerns, J. He, J. Fee, C. Tinson, J. Shi, S. March, M. Jain, S.L. Suib, Enhanced visible-light-assisted peroxymonosulfate activation on cobalt-doped mesoporous iron oxide for orange II degradation, Applied Catalysis B: Environmental, (2019) 118332.

[29] Y.-Y. Ahn, H. Bae, H.-I. Kim, S.-H. Kim, J.-H. Kim, S.-G. Lee, J. Lee, Surface-loaded metal nanoparticles for peroxymonosulfate activation: Efficiency and mechanism reconnaissance, Applied Catalysis B: Environmental, 241 (2019) 561-569.

[30] J. Rodríguez-Chueca, S. Guerra-Rodríguez, J.M. Raez, M.-J. López-Muñoz, E. Rodríguez, Assessment of different iron species as activators of S2O82- and HSO5- for inactivation of wild bacteria strains, Applied Catalysis B: Environmental, 248 (2019) 54-61.

[31] M.M. Mian, G. Liu, B. Fu, Y. Song, Facile synthesis of sludge-derived MnOx-N-biochar as an efficient catalyst for peroxymonosulfate activation, Applied Catalysis B: Environmental, 255 (2019) 117765.

[32] C. Alexopoulou, A. Petala, Z. Frontistis, C. Drivas, S. Kennou, D.I. Kondarides, D. Mantzavinos, Copper phosphide and persulfate salt: A novel catalytic system for the degradation of aqueous phase micro-contaminants, Applied Catalysis B: Environmental, 244 (2019) 178-187.

[33] P.L. Smedley, D.G. Kinniburgh, Molybdenum in natural waters: A review of occurrence, distributions and controls, Applied Geochemistry, 84 (2017) 387-432.

[34] A. Giussani, J.O. Nriagu, Molybdenum in the Environment and its Relevance for Animal and Human Health, Encyclopedia of Environmental Health, Elsevier, Burlington, 2011, pp. 840-846.

[35] S.J. Morrison, P.S. Mushovic, P.L. Niesen, Early Breakthrough of Molybdenum and Uranium in a Permeable Reactive Barrier, Environmental Science & Technology, 40 (2006) 2018-2024.

[36] S.J. Morrison, R.R. Spangler, Extraction of uranium and molybdenum from aqueous solutions: a survey of industrial materials for use in chemical barriers for uranium mill tailings remediation,

Environmental Science & Technology, 26 (1992) 1922-1931.

[37] M. Zhang, E.J. Reardon, Removal of B, Cr, Mo, and Se from Wastewater by Incorporation into Hydrocalumite and Ettringite, Environmental Science & Technology, 37 (2003) 2947-2952.

[38] W. Wei, Q. Tian, H. Sun, P. Liu, Y. Zheng, M. Fan, J. Zhuang, Efficient visible-light-driven photocatalytic H2 evolution over MoO2-C/CdS ternary heterojunction with unique interfacial microstructures, Applied Catalysis B: Environmental, 260 (2020) 118153.

[39] C. Fang, P. Yan, Z. Ren, Y. Wang, X. Cai, X. Li, G. Han, Multifunctional MoO2-ICG nanoplatform for 808nm-mediated synergetic photodynamic/photothermal therapy, Applied Materials Today, 15 (2019) 472-481.

[40] T. Anh Tran, K. Krishnamoorthy, Y.W. Song, S.K. Cho, S.J. Kim, Toxicity of Nano Molybdenum Trioxide toward Invasive Breast Cancer Cells, ACS Applied Materials & Interfaces, 6 (2014) 2980-2986.

[41] G. Song, J. Shen, F. Jiang, R. Hu, W. Li, L. An, R. Zou, Z. Chen, Z. Qin, J. Hu, Hydrophilic Molybdenum Oxide Nanomaterials with Controlled Morphology and Strong Plasmonic Absorption for Photothermal Ablation of Cancer Cells, ACS Applied Materials & Interfaces, 6 (2014) 3915-3922.

[42] G. Song, J. Hao, C. Liang, T. Liu, M. Gao, L. Cheng, J. Hu, Z. Liu, Degradable Molybdenum Oxide Nanosheets with Rapid Clearance and Efficient Tumor Homing Capabilities as a Therapeutic Nanoplatform, Angewandte Chemie International Edition, 55 (2016) 2122-2126.

[43] H. Du, X. Xie, Q. Zhu, L. Lin, Y.-F. Jiang, Z.-K. Yang, X. Zhou, A.-W. Xu, Metallic MoO2 cocatalyst significantly enhances visible-light photocatalytic hydrogen production over MoO2/Zn0.5Cd0.5S heterojunction, Nanoscale, 7 (2015) 5752-5759.

[44] H. Zheng, J. Bao, Y. Huang, L. Xiang, Faheem, B. Ren, J. Du, M.N. Nadagouda, D.D. Dionysiou, Efficient degradation of atrazine with porous sulfurized Fe2O3 as catalyst for peroxymonosulfate activation, Applied Catalysis B: Environmental, 259 (2019) 118056.

[45] J. Wang, S. Wang, Activation of persulfate (PS) and peroxymonosulfate (PMS) and application for the degradation of emerging contaminants, Chemical Engineering Journal, 334 (2018) 1502-1517.

[46] F. Ghanbari, M. Moradi, Application of peroxymonosulfate and its activation methods for degradation of environmental organic pollutants: Review, Chemical Engineering Journal, 310 (2017) 41-62.

[47] J. Li, Y. Wan, Y. Li, G. Yao, B. Lai, Surface Fe(III)/Fe(II) cycle promoted the degradation of atrazine by peroxymonosulfate activation in the presence of hydroxylamine, Applied Catalysis B: Environmental, 256 (2019) 117782.

[48] C. Liu, L. Chen, D. Ding, T. Cai, From rice straw to magnetically recoverable nitrogen doped biochar: Efficient activation of peroxymonosulfate for the degradation of metolachlor, Applied Catalysis B: Environmental, 254 (2019) 312-320.

[49] X. Duan, H. Sun, Z. Shao, S. Wang, Nonradical reactions in environmental remediation processes: Uncertainty and challenges, Applied Catalysis B: Environmental, 224 (2018) 973-982.

[50] Y. Wang, S. Chen, Droplets impact on textured surfaces: Mesoscopic simulation of spreading dynamics, Applied Surface Science, 327 (2015) 159-167.

[51] G.P. Anipsitakis, D.D. Dionysiou, Radical Generation by the Interaction of Transition Metals with Common Oxidants, Environmental Science & Technology, 38 (2004) 3705-3712.

[52] Y. Yao, C. Lian, G. Wu, Y. Hu, F. Wei, M. Yu, S. Wang, Synthesis of "sea urchin"-like carbon nanotubes/porous carbon superstructures derived from waste biomass for treatment of various

contaminants, Applied Catalysis B: Environmental, 219 (2017) 563-571.

[53] W.-D. Oh, Z. Dong, T.-T. Lim, Generation of sulfate radical through heterogeneous catalysis for organic contaminants removal: Current development, challenges and prospects, Applied Catalysis B: Environmental, 194 (2016) 169-201.

[54] F. Wang, J. Jiang, K. Wang, Q. Zhai, F. Long, P. Liu, J. Feng, H. Xia, J. Ye, J. Li, J. Xu, Hydrotreatment of lipid model for diesel-like alkane using nitrogen-doped mesoporous carbon-supported molybdenum carbide, Applied Catalysis B: Environmental, 242 (2019) 150-160.

[55] Y. Qian, X. Zhou, Y. Zhang, P. Sun, W. Zhang, J. Chen, X. Guo, X. Zhang, Performance of α-methylnaphthalene degradation by dual oxidant of persulfate/calcium peroxide: Implication for ISCO, Chemical Engineering Journal, 279 (2015) 538-546.

[56] Y. Cui, Z. Ding, Y. Sun, Y. Yi, F. Xu, Q. Zhang, W. Wang, A theoretical study of OH radical-initiated atmospheric oxidation of 1-chloronaphthalene, Chemical Physics Letters, 699 (2018) 40-47.

[57] W. Zhang, J. Chen, B. Pan, Q. Zhang, Cooperative adsorption behaviours of 1-naphthol and 1-naphthylamine onto nonpolar macroreticular adsorbents, Reactive and Functional Polymers, 66 (2006) 485-493.

[58] X. Wang, C. Chen, J. Li, X. Wang, Ozone degradation of 1-naphthol on multiwalled carbon nanotubes/iron oxides and recycling of the adsorbent, Chemical Engineering Journal, 262 (2015) 1303-1310.

[59] W. Feng, Y. Wang, K. W, Z. Zhai, W. Jin, Path of photocatalytic degradation of 1-naphthol by nanocrystalline TiO2, Journal of Tianjin University, 42 (2009) 258-266.

[60] Z. Huang, Q. Zhang, W. Wang, Mechanical and kinetic study on gas-phase formation of dinitro-naphthalene from 1- and 2-nitronaphthalene, Chemosphere, 156 (2016) 101-110.

[61] H.L. So, W. Chu, Y.H. Wang, Naphthalene degradation by Fe2+/Oxone/UV – Applying an unconventional kinetics model and studying the reaction mechanism, Chemosphere, 218 (2019) 110-118.

[62] B.A.M. Bandowe, H. Meusel, Nitrated polycyclic aromatic hydrocarbons (nitro-PAHs) in the environment – A review, Science of The Total Environment, 581-582 (2017) 237-257.

[63] X. Li, Z. Ao, J. Liu, H. Sun, A.I. Rykov, J. Wang, Topotactic Transformation of Metal–Organic Frameworks to Graphene-Encapsulated Transition-Metal Nitrides as Efficient Fenton-like Catalysts, ACS Nano, 10 (2016) 11532-11540.

[64] S. Indrawirawan, H. Sun, X. Duan, S. Wang, Nanocarbons in different structural dimensions (0–3D) for phenol adsorption and metal-free catalytic oxidation, Applied Catalysis B: Environmental, 179 (2015) 352-362.

[65] T. Zhang, H. Zhu, J.-P. Croué, Production of Sulfate Radical from Peroxymonosulfate Induced by a Magnetically Separable CuFe2O4 Spinel in Water: Efficiency, Stability, and Mechanism, Environmental Science & Technology, 47 (2013) 2784-2791.

[66] Y. Wang, C. Liu, Y. Zhang, W. Meng, B. Yu, S. Pu, D. Yuan, F. Qi, B. Xu, W. Chu, Sulfate radical-based photo-Fenton reaction derived by CuBi2O4 and its composites with α-Bi2O3 under visible light irradiation: Catalyst fabrication, performance and reaction mechanism, Applied Catalysis B: Environmental, 235 (2018) 264-273.

[67] R. Yuan, L. Hu, P. Yu, H. Wang, Z. Wang, J. Fang, Nanostructured Co3O4 grown on nickel foam: An efficient and readily recyclable 3D catalyst for heterogeneous peroxymonosulfate activation,

Chemosphere, 198 (2018) 204-215.

[68] M. Zhang, C. Wang, C. Liu, L. Rui, J. Li, X. Sun, J. Shen, W. Han, L. Wang, Metal-organic framework derived Co3O4/C@SiO2 yolk-shell nanoreactors with enhanced catalytic performance, Journal of Materials Chemistry A, 6 (2018).

[69] G.V. Buxton, C.L. Greenstock, W.P. Helman, A.B. Ross, Critical Review of rate constants for

reactions of hydrated electrons, hydrogen atoms and hydroxyl radicals (·OH/·O− in Aqueous Solution,

Journal of Physical and Chemical Reference Data, 17 (1988) 513-886.

[70] P. Neta, R.E. Huie, A.B. Ross, Rate Constants for Reactions of Inorganic Radicals in Aqueous Solution, Journal of Physical and Chemical Reference Data, 17 (1988) 1027-1284.

[71] X. Chen, W.-D. Oh, Z.-T. Hu, Y.-M. Sun, R.D. Webster, S.-Z. Li, T.-T. Lim, Enhancing sulfacetamide degradation by peroxymonosulfate activation with N-doped graphene produced through delicately-controlled nitrogen functionalization via tweaking thermal annealing processes, Applied Catalysis B: Environmental, 225 (2018) 243-257.

[72] D.L. Ball, J.O. Edwards, The Kinetics and Mechanism of the Decomposition of Caro's Acid. I, Journal of the American Chemical Society, 78 (1956) 1125-1129.

[73] H.A. Schwarz, R.W. Dodson, Reduction potentials of CO2- and the alcohol radicals, The Journal of Physical Chemistry, 93 (1989) 409-414.

[74] G.R. Peyton, O.J. Bell, E. Girin, M.H. LeFaivre, Reductive Destruction of Water Contaminants during Treatment with Hydroxyl Radical Processes, Environmental Science & Technology, 29 (1995) 1710-1712.

[75] L. Tang, Y. Liu, J. Wang, G. Zeng, Y. Deng, H. Dong, H. Feng, J. Wang, B. Peng, Enhanced activation process of persulfate by mesoporous carbon for degradation of aqueous organic pollutants: Electron transfer mechanism, Applied Catalysis B: Environmental, 231 (2018) 1-10.

[76] R. Zhuang, S. Yao, X. Shen, T. Li, Hydrothermal synthesis of mesoporous MoO2 nanospheres as sulfur matrix for lithium sulfur battery, Journal of Electroanalytical Chemistry, 833 (2019) 441-448.

[77] G. Fang, W. Wu, C. Liu, D.D. Dionysiou, Y. Deng, D. Zhou, Activation of persulfate with vanadium species for PCBs degradation: A mechanistic study, Applied Catalysis B-Environmental, 202 (2017) 1-11.

[78] J.E. Silveira, W.S. Paz, P. Garcia-Muñoz, J.A. Zazo, J.A. Casas, UV-LED/ilmenite/persulfate for azo dye mineralization: The role of sulfate in the catalyst deactivation, Applied Catalysis B: Environmental, 219 (2017) 314-321.

[79] T.D. Minh, M.C. Ncibi, V. Srivastava, S.K. Thangaraj, J. Jänis, M. Sillanpää, Gingerbread ingredient-derived carbons-assembled CNT foam for the efficient peroxymonosulfate-mediated degradation of emerging pharmaceutical contaminants, Applied Catalysis B: Environmental, 244 (2019) 367-384.

[80] H. Liu, T.A. Bruton, W. Li, J.V. Buren, C. Prasse, F.M. Doyle, D.L. Sedlak, Oxidation of Benzene by Persulfate in the Presence of Fe(III)- and Mn(IV)-Containing Oxides: Stoichiometric Efficiency and Transformation Products, Environmental Science & Technology, 50 (2016) 890-898.

[81] J.C. Espinosa, P. Manickam-Periyaraman, F. Bernat-Quesada, S. Sivanesan, M. Álvaro, H. García, S. Navalón, Engineering of activated carbon surface to enhance the catalytic activity of supported

cobalt oxide nanoparticles in peroxymonosulfate activation, Applied Catalysis B: Environmental, 249 (2019) 42-53.

[82] H. Jia, S. Zhao, Y. Shi, L. Zhu, C. Wang, V.K. Sharma, Transformation of Polycyclic Aromatic Hydrocarbons and Formation of Environmentally Persistent Free Radicals on Modified Montmorillonite: The Role of Surface Metal Ions and Polycyclic Aromatic Hydrocarbon Molecular Properties, Environmental Science & Technology, 52 (2018) 5725-5733.

[83] H. Jia, S. Zhao, G. Nulaji, K. Tao, F. Wang, V.K. Sharma, C. Wang, Environmentally Persistent Free Radicals in Soils of Past Coking Sites: Distribution and Stabilization, Environmental Science & Technology, 51 (2017) 6000-6008.

[84] H. Jia, S. Zhao, K. Zhu, D. Huang, L. Wu, X. Guo, Activate persulfate for catalytic degradation of adsorbed anthracene on coking residues: Role of persistent free radicals, Chemical Engineering Journal, 351 (2018) 631-640.

[85] B. Jiang, Y. Yao, R. Xie, D. Dai, W. Lu, W. Chen, L. Zhang, Enhanced generation of reactive oxygen species for efficient pollutant elimination catalyzed by hemin based on persistent free radicals, Applied Catalysis B: Environmental, 183 (2016) 291-297.

Figures

(g) Nano MoO$_2$ + PMS processing

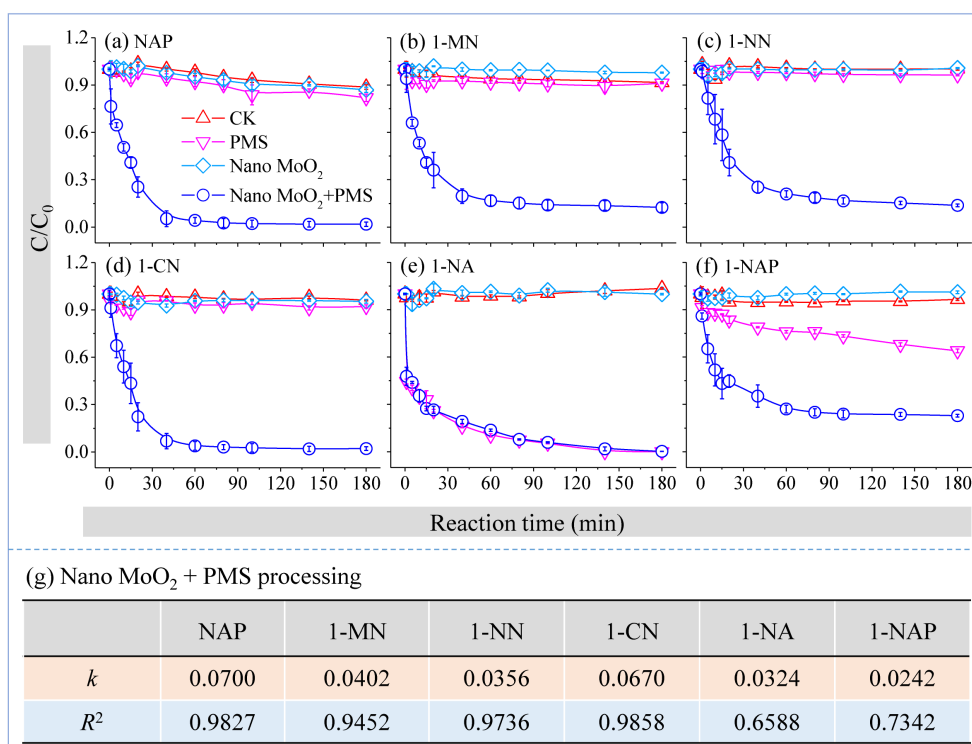|	NAP	1-MN	1-NN	1-CN	1-NA	1-NAP
k	0.0700	0.0402	0.0356	0.0670	0.0324	0.0242
R^2	0.9827	0.9452	0.9736	0.9858	0.6588	0.7342

Figure 1 Activation of PMS by nano MoO$_2$ for the degradation of contaminants. (a): Naphthalene (NAP), (b): 1-Methylnaphthalene (1-MN), (c): 1-Nitronaphthalene (1-NN), (d): 1-Chloronaphthalene (1-CN), (e): 1-Naphthylamine (1-NA), (f): 1-Naphthol (1-NAP). (g) Reaction rate constant k and correlation coefficient of each pollutant, obtained by data fitting with a pseudo-first-order kinetic model. CK indicates the control treatment without PMS and Nano MoO$_2$. Reaction conditions: Nano MoO$_2$ loading = 0.05 g L^{-1}, [PMS]$_0$ = 4.0 mmol L^{-1}, [contaminants]$_0$ = 1 mg L^{-1}, pH = 4.4 and 25°C.
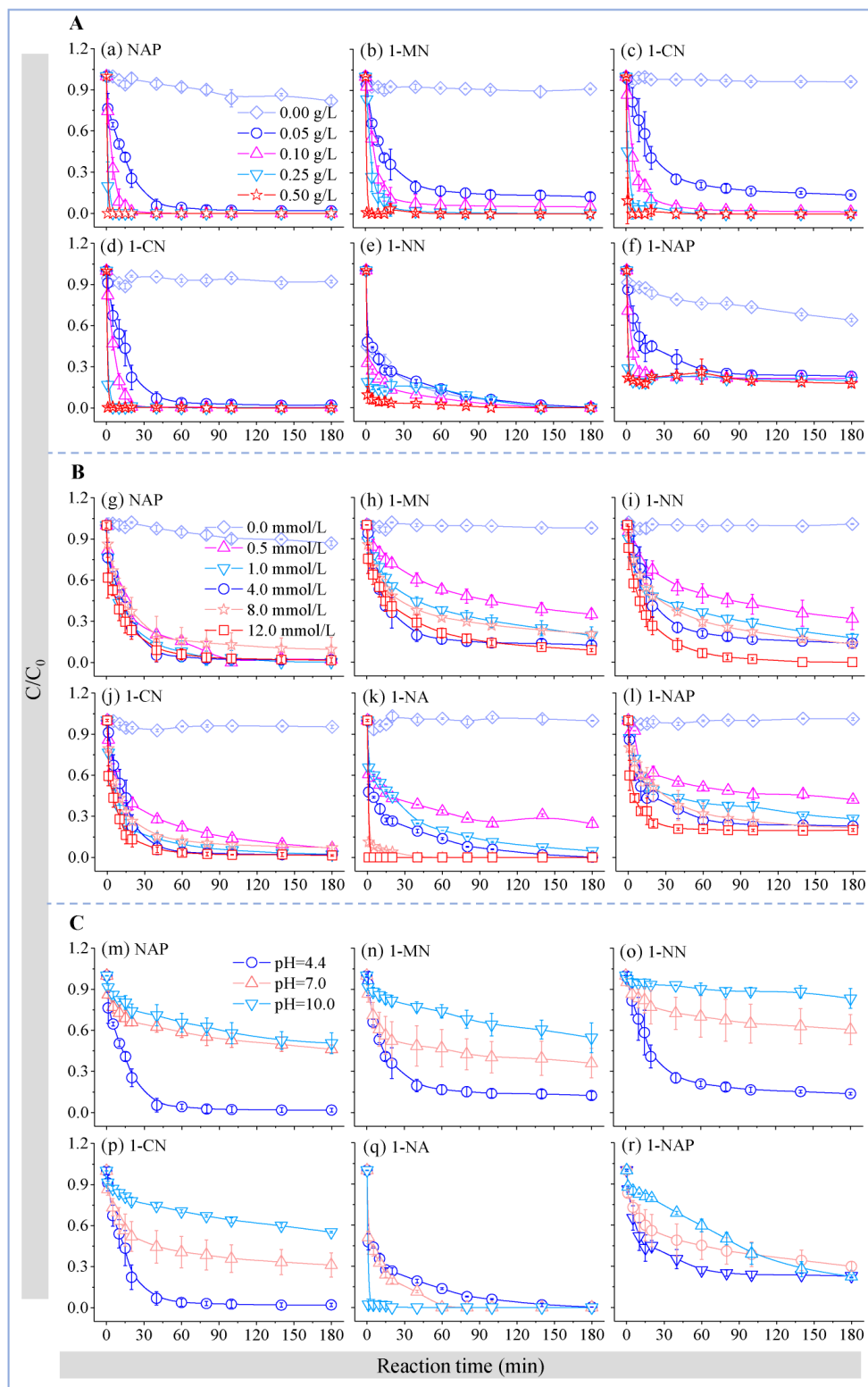
Figure 2 Effects of A: nano MoO_2 loading, B: PMS concentration and C: initial pH on contaminants degradation. (a), (g) and (m): Naphthalene, (b), (h) and (n): 1-Methylnaphthalene, (c), (i) and (o): 1-Nitronaphthalene, (d), (j) and (p): 1-Chloronaphthalene, (e), (k) and (q): 1-Naphthylamine, (f), (l) and (r): 1-Naphthol. Reaction conditions: Nano MoO_2 loading = 0.00 - 0.05 g L^{-1}, $[PMS]_0$ = 0.0 - 12.0
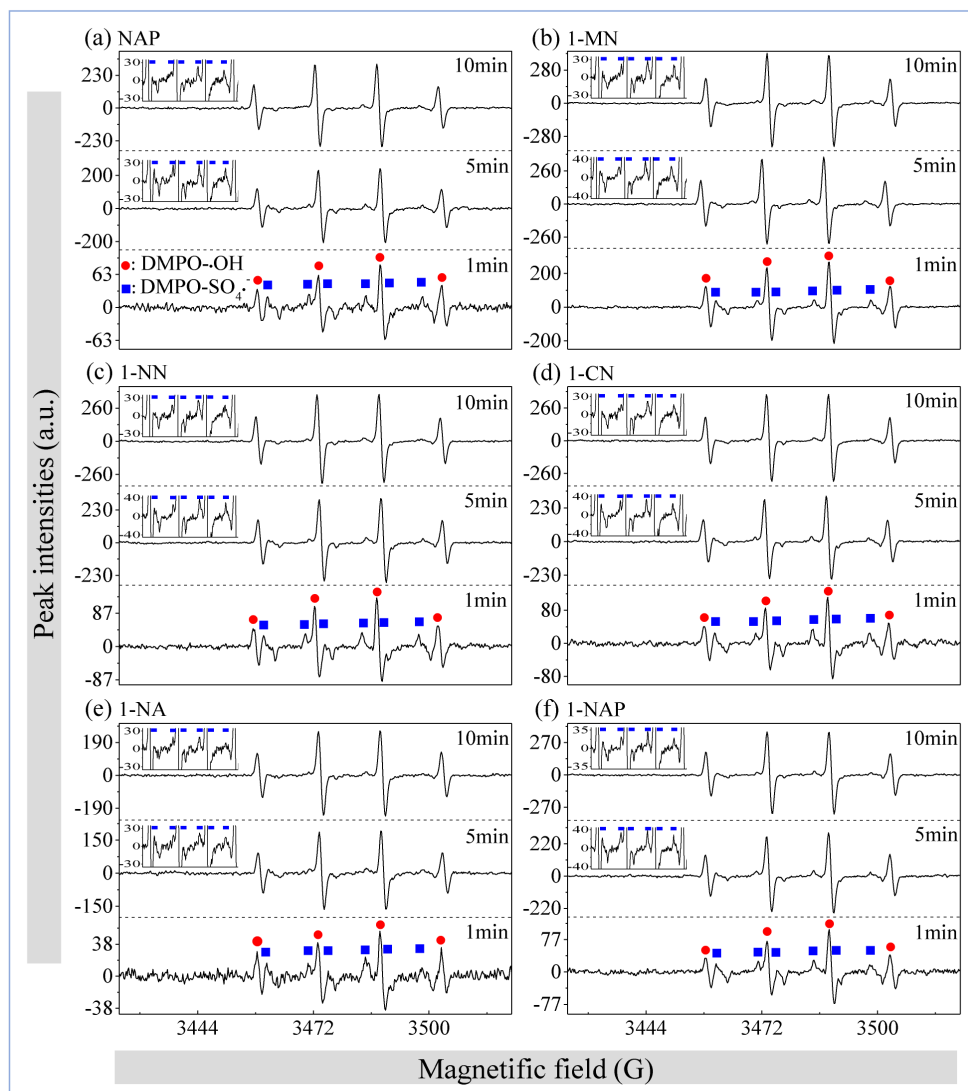
mmol L^{-1}, pH = 4.4 - 10.0, [contaminants]$_0$ = 1 mg L^{-1}, 25°C.

Figure 3 Determination of SO$_4^{\bullet-}$ and $^\bullet$OH by EPR in the nano MoO$_2$/PMS system. (a): Naphthalene, (b): 1-Methylnaphthalene, (c): 1-Nitronaphthalene, (d): 1-Chloronaphthalene, (e): 1-Naphthylamine, (f): 1-Naphthol. Reaction conditions: Nano MoO$_2$ loading = 0.05 g L^{-1}, [PMS]$_0$ = 4.0 mmol L^{-1}, pH = 4.4, [contaminants]$_0$ = 1 mg L^{-1}, [DMPO]$_0$ = 100 mmol L^{-1}, 25°C.
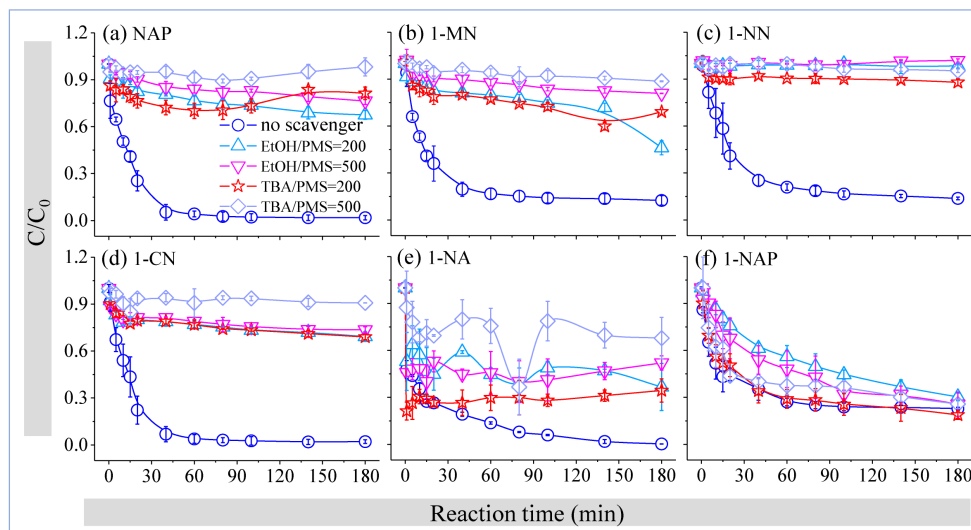
Figure 4 Effects of scavengers (TBA and EtOH) on the degradation of contaminants, at different molar ratios with PMS in the nano MoO$_2$/PMS system. (a): Naphthalene, (b): 1-Methylnaphthalene, (c): 1-Nitronaphthalene, (d): 1-Chloronaphthalene, (e): 1-Naphthylamine, (f): 1-Naphthol. Reaction conditions: Nano MoO$_2$ loading = 0.05 g L^{-1}, [PMS]$_0$ = 4.0 mmol L^{-1}, pH = 4.4, [contaminants]$_0$ = 1 mg L^{-1}, [TBA]$_0$ ([EtOH]$_0$)/[PMS]$_0$ = 200 and 500 ~~mmol L^{-1}~~, 25°C. **I would delete the datum of 1-NA at around 75 min (outlier)**
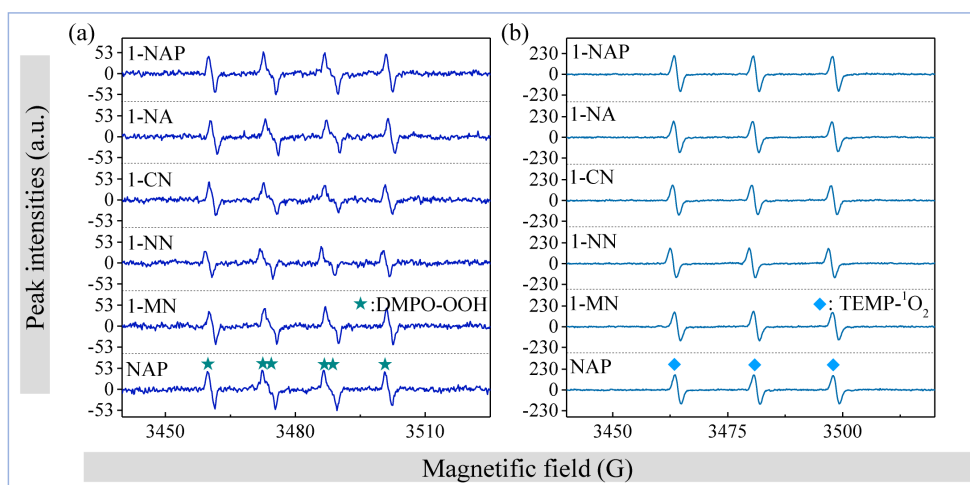
Figure 5 Identification of (a) O$_2^{\bullet-}$ and (b) ^{1}O$_2$ by EPR in the nano MoO$_2$/PMS system. Reaction conditions: Nano MoO$_2$ loading = 0.05 g L^{-1}, [PMS]$_0$ = 4.0 mmol L^{-1}, pH = 4.4, [contaminants]$_0$ = 1 mg L^{-1}, [DMPO]$_0$ = 100 mmol L^{-1}, [TEMP]$_0$ = 30 mmol L^{-1}, 25°C.
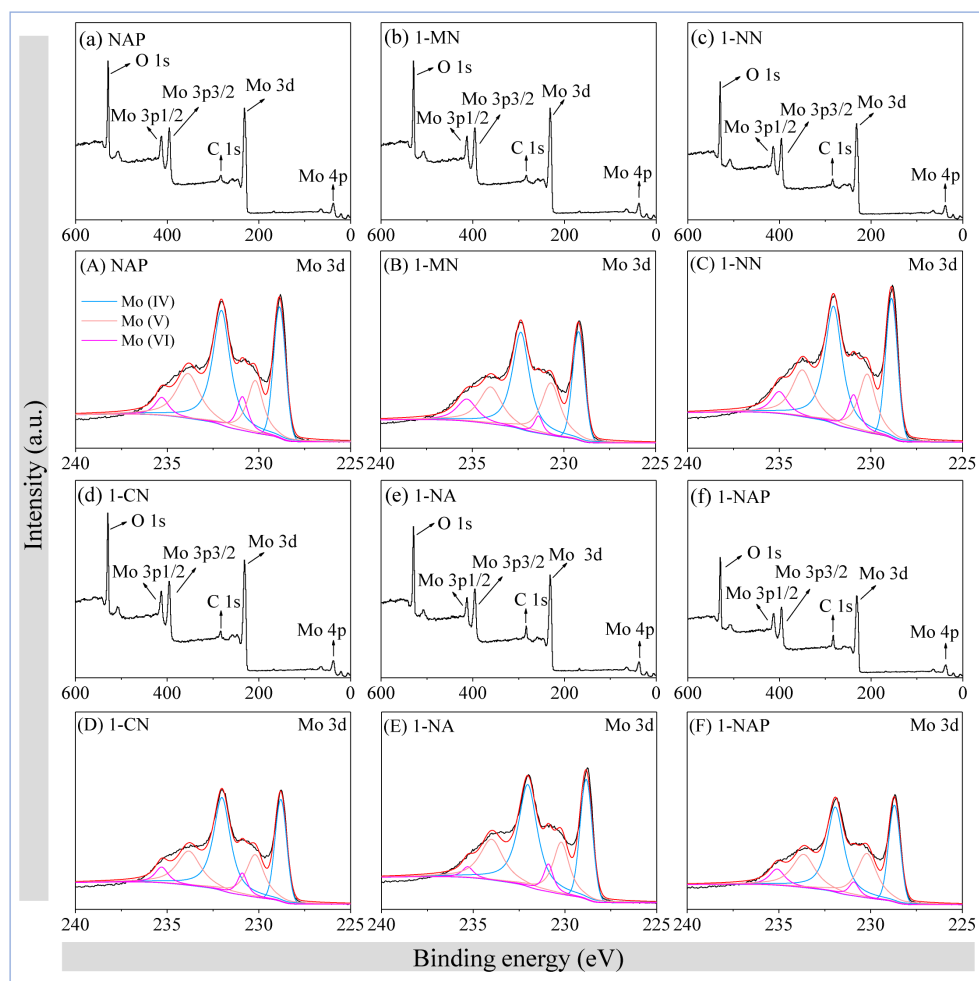
Figure 6 XPS analysis of the change of the valence states of Mo after the reaction. (a) - (f): Full-range scan of the samples; (A) - (F): Mo 3d core level. (a) and (A): Naphthalene/Nano MoO_2/PMS system, (b) and (B): 1-Methylnaphthalene/Nano MoO_2/PMS system, (c) and (C): 1-Nitronaphthalene/Nano MoO_2/PMS system, (d) and (D): 1-Chloronaphthalene/Nano MoO_2/PMS system, (e) and (E): 1-Naphthylamine/Nano MoO_2/PMS system, (f) and (F): 1-Naphthol/Nano MoO_2/PMS system.
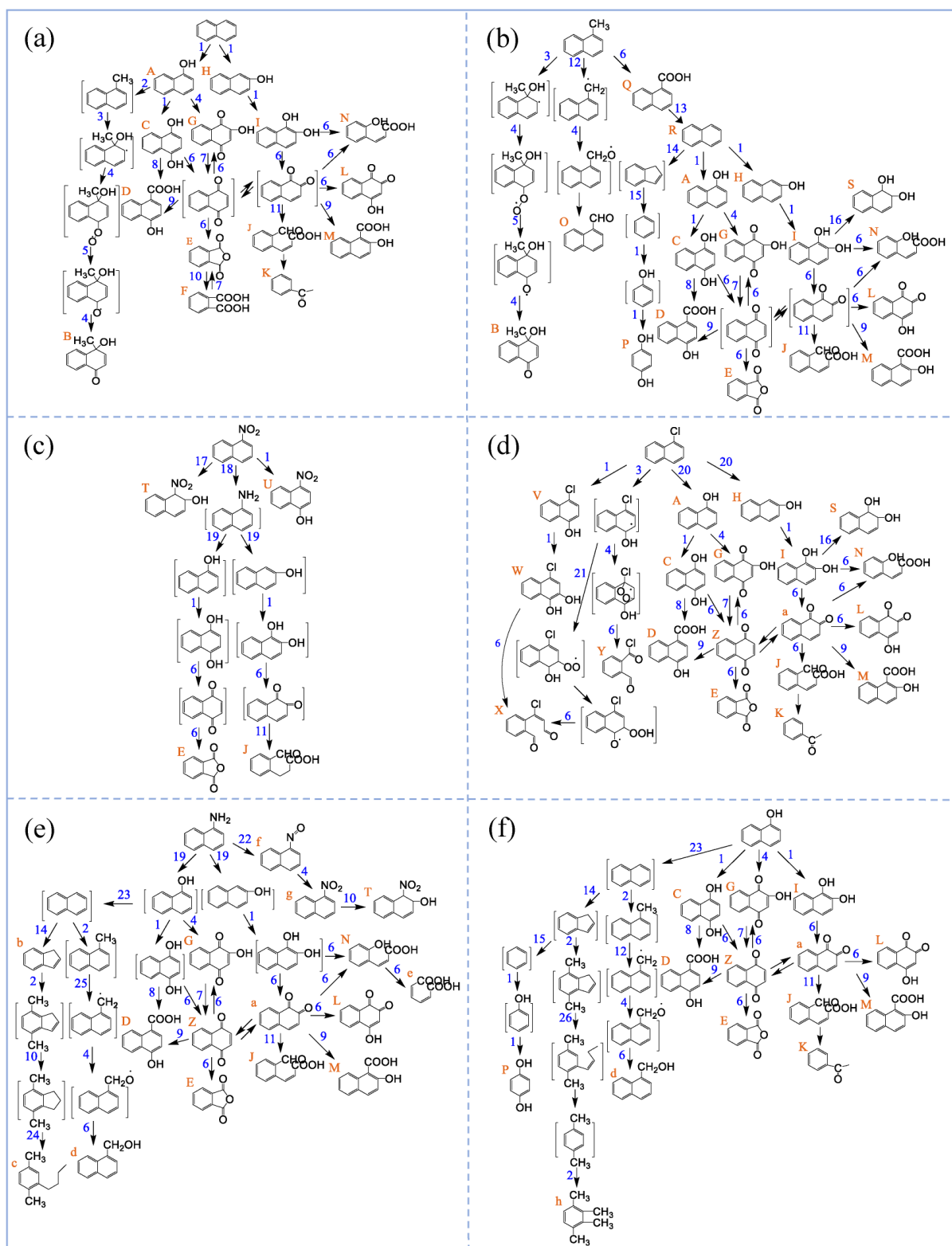
Figure 7 Proposed pathways for contaminants degradation in the nano MoO$_2$/PMS system. (a): Naphthalene; (b): 1-Methylnaphthalene; (c): 1-Nitronaphthalene; (d): 1-Chloronaphthalene; (e): 1-Naphthylamine; (f): 1-Naphthol. A 1-naphthol C$_{10}$H$_8$O; B 4-hydroxy-4-methylnaphthalen-1(4H)-one C$_{11}$H$_{10}$O$_2$; C 1,4-dihydroxy-naphthalene C$_{10}$H$_8$O$_2$; D 4-hydroxy-1-naphthoic acid C$_{11}$H$_8$O$_3$; E

o-phthalic anhydride $C_8H_4O_3$; F phthalic acid $C_8H_6O_4$; G 2-hydroxy-1,4-naphoquinone $C_{10}H_6O_3$; H 2-naphthol $C_{10}H_8O$; I 1,2-dihydroxy-naphthalene $C_{10}H_8O_2$; J carboxyl cinnamaldehydes $C_{10}H_8O_3$; K acetophenone C_8H_8O; L 4-hydroxy-1,2-naphoquinone $C_{10}H_6O_3$; M 2-hydroxy-1-naphthoic acid $C_{11}H_8O_3$; N 2-hydroxycinnamic acid $C_9H_8O_3$; O 1-naphthaldehyde $C_{11}H_8O$; P hydroquinone $C_6H_6O_2$; Q 1-naphthoic acid $C_{11}H_8O_2$; R naphthalene $C_{10}H_8$; S 1,2-dihydro-1,2-dihydroxynaphthalene $C_{10}H_{10}O_2$; T 1-nitro-1,2-dihydronaphthalen-2-ol $C_{10}H_9NO_3$; U 4-hydroxy-1-nitronaphthalene $C_{10}H_7NO_3$; V 4-chloronaphthalen-1-ol $C_{10}H_7ClO$; W 4-chloronaphthalene-1,2-diol $C_{10}H_7ClO_2$; X (E)-2-(1-chloro-3-oxoprop-1-en-1-yl)benzaldehyde $C_{10}H_7ClO_2$; Y 2-formylbenzoyl chloride $C_8H_5ClO_2$; Z 1,4-naphthoquinone $C_{10}H_6O_2$; a 1,2-naphthoquinone $C_{10}H_6O_2$; b indene C_9H_8; c 2-butyl-1,4-dimethylbenzene $C_{12}H_{18}$; d 1-naphthylmethanol $C_{11}H_{10}O$; e (2Z,4Z)-hexa-2,4-dienedioic acid $C_6H_6O_4$; f 1-nitrosonaphthalene $C_{10}H_7NO$; g 1-nitronaphthalene $C_{10}H_7NO_2$; h tetramethylbenzene $C_{10}H_{14}$. 1 Hydroxylation; 2 Alkyl substitution; 3 Naphthalene-ring attack; 4 [O]; 5 HO_2; 6 Free radical oxidation; 7 H_2O; 8 Carbonylation; 9 Hydroformylation-like; 10 H; 11 Oxidation + ring-opening; 12 Attack to the methyl carbon atoms; 13 Decarboxylation; 14 Oxidative demethylation; 15 Ring opening + chain fragmentation; 16 Hydrogenation; 17 Hydroxylation + hydrogenation; 18 Attack to the nitro nitrogen atom; 19 Hydrogen bonding interaction; 20 Hydroxyl substitution; 21 O_2 addition; 22 Attack to the amino functional group; 23 Dehydroxylation; 24 Ring opening; 25 Attack to the methyl carbon atoms; 26 H + ring opening.
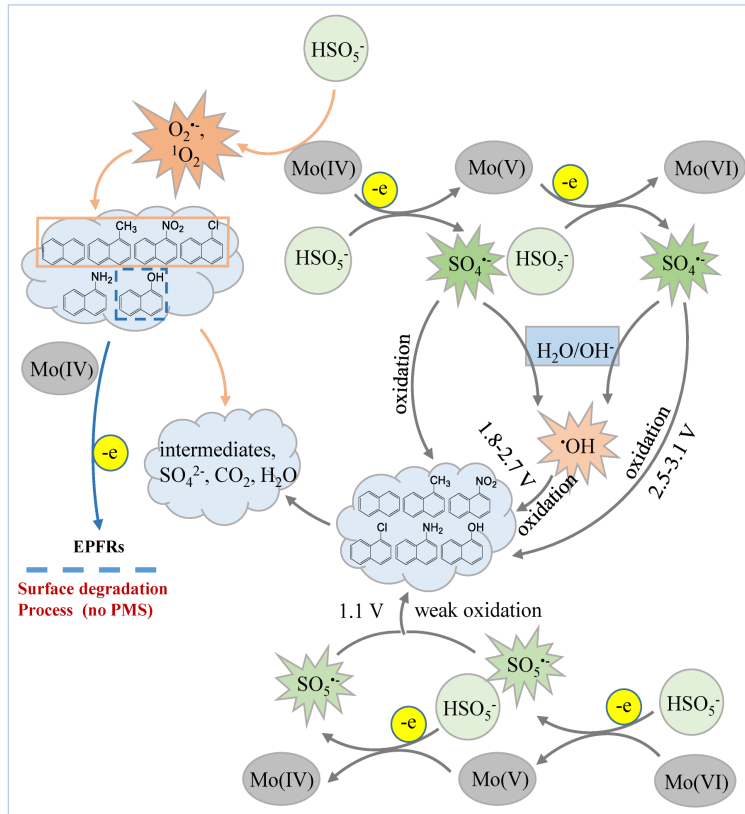
Figure 9 The possible mechanism of PMS activation and naphthalene and derivatives degradation in the nano MoO_2/PMS system.

Tab. 1 Reaction rate constants k and correlation coefficients for the effects of nano MoO_2 loading, PMS concentration and initial pH on contaminants degradation, obtained by data fitting with a pseudo-first-order kinetic model. NAP: Naphthalene, 1-MN: 1-Methylnaphthalene, 1-NN: 1-Nitronaphthalene, 1-CN: 1-Chloronaphthalene, 1-NA: 1-Naphthylamine, 1-NAP: 1-Naphthol.

			NAP	1-MN	1-NN	1-CN	1-NA	1-NAP
Nano MoO_2 loading (g/L)	0.05	k	0.0700	0.0402	0.0356	0.0670	0.0324	0.0242
		R^2	0.9827	0.9452	0.9736	0.9858	0.6588	0.7342
	0.10	k	0.2086	0.0681	0.0378	0.2136	0.0452	0.1292
		R^2	0.9853	0.8053	0.8764	0.9244	0.6220	0.9266
	0.25	k	1.1299	0.0991	0.5829	1.0028	0.2963	0.2625
		R^2	0.9859	0.8341	0.9911	0.9555	0.1054	0.3109
	0.50	k	unavailable	0.9938	unavailable	unavailable	0.4389	unavailable
		R^2	—	0.3300	—	—	0.1691	—
PMS concentration (mmol/L)	0.5	k	0.0388	0.0116	0.0146	0.0306	0.0179	0.0150
		R^2	0.9253	0.9168	0.8594	0.7861	0.5764	0.5483
	1.0	k	0.0504	0.0194	0.0219	0.0491	0.0289	0.0197
		R^2	0.9587	0.9051	0.8226	0.8539	0.8864	0.7321
	4.0	k	0.0700	0.0402	0.0356	0.0670	0.0324	0.0242
		R^2	0.9827	0.9452	0.9736	0.9858	0.6588	0.7342
	8.0	k	0.0418	0.0227	0.0248	0.0446	0.2147	0.0214
		R^2	0.9771	0.8601	0.8914	0.9085	0.3485	0.8736
	12.0	k	0.0548	0.0280	0.0280	0.0679	unavailable	0.0328
		R^2	0.9548	0.8667	0.9572	0.9063	—	0.6732
Initial pH	4.4	k	0.0700	0.0402	0.0356	0.0670	0.0324	0.0242
		R^2	0.9827	0.9452	0.9736	0.9858	0.6588	0.7342
	7.0	k	0.0098	0.0164	0.0074	0.0188	0.0462	0.0157
		R^2	0.6477	0.6773	0.8045	0.8078	0.8173	0.7657
	10.0	k	0.0076	0.0054	0.0014	0.0064	unavailable	0.0074
		R^2	0.7689	0.7443	0.5156	0.7463	—	0.8193

Tab. 2 Degradation fraction and standard deviation of nano MoO_2 when it was used to degrade contaminants in 4 consecutive cycles. NAP: Naphthalene, 1-MN: 1-Methylnaphthalene, 1-NN: 1-Nitronaphthalene, 1-CN: 1-Chloronaphthalene, 1-NA: 1-Naphthylamine, 1-NAP: 1-Naphthol.

		NAP	1-MN	1-NN	1-CN	1-NA	1-NAP
1st	$(C_0-C)/C_0$	0.9818	0.8752	0.8623	0.9787	0.9974	0.7716
	σ	0.0141	0.0299	0.0085	0.0122	0.0008	0.0081
2nd	$(C_0-C)/C_0$	0.9141	0.5717	0.3573	0.4616	1.0000	0.5450
	σ	0.0157	0.0393	0.0965	0.1650	0.0000	0.1508
3rd	$(C_0-C)/C_0$	0.6064	0.3968	0.2291	0.4702	1.0000	0.5409
	σ	0.1132	0.0662	0.1012	0.1009	0.0000	0.1233
4th	$(C_0-C)/C_0$	0.7002	0.4431	0.2439	0.5624	1.0000	0.6739
	σ	0.0564	0.0328	0.0842	0.1394	0.0000	0.0770